Tropical rainforest above Ground Biomass and Carbon Stock Estimation for Upper and Lower canopies Using Terrestrial Laser Scanner and Canopy Height Model from Unmanned Aerial Vehicle (UAV) Imagery in Ayer-Hitam, Malaysia

YUVENAL PANTALEO MTUI
FEBRUARY, 2017

SUPERVISORS:
Dr. Yousif A. Hussin
Drs. E. H. Kloosterman

Tropical rainforest above Ground Biomass and Carbon Stock Estimation for Upper and Lower canopies Using Terrestrial Laser Scanner and Canopy Height Model from Unmanned Aerial Vehicle (UAV) Imagery in Ayer-Hitam, Malaysia

YUVENAL PANTALEO MTUI

Enschede, The Netherlands, February, 2017

Thesis submitted to the Faculty of Geo-Information Science and Earth Observation of the University of Twente in partial fulfilment of the requirements for the degree of Master of Science in Geo-information Science and Earth Observation.

Specialization: Natural Resources Management

SUPERVISORS:
Dr. Yousif A. Hussin
Drs. E. H. Kloosterman

THESIS ASSESSMENT BOARD:
Prof.dr. A.D. Nelson (Chair)
Dr. T. Kauranne (External Examiner, Lappeenranta University of Technology, Finland)

ABSTRACT

Tropical forests play a major role to sequester and store large amounts of carbon which play a key role in the global carbon budget and an important natural control of climate change. The carbon stored in the aboveground living biomass of trees is typically the largest pool and the most directly impacted by deforestation and degradation which are among of the drivers of climate change. To control the impact of climate change, REDD+ program and its MRV mechanism have been established under UNFCCC.

There is a great need for a cost-effective and accurate method to assess the complex multi-layered tropical rain-forest parameters for estimating above-ground biomass (AGB)/carbon stock. The tree height and Diameter at Breast Height (DBH) are important forest parameters required as inputs for biomass estimation equation and can be obtained through various methods such as direct field measurement. Moreover, measuring tree height and DBH by field surveying is time-consuming, limited to inaccessible areas and rather expensive. The advancement of remote sensing technology, various datasets have been used to assess AGB including airborne LiDAR or sometimes called Airborne Laser Scanner (ALS) but not always available and expensive to acquire for regular monitoring. The emergent of Unmanned Aerial Vehicle (UAV) and Terrestrial Laser Scanner (TLS) technologies operate from air and ground respectively can provide accurate information of upper and lower canopy layers at a reasonable cost for regular monitoring of carbon stock. However, both associated with limitation of foliage coverage in the complex multi-layer tropical forest which can underestimate AGB estimation when used separately. This study aimed at establishing a cost-effective method that ensures reasonable accuracy for regular assessment of tropical rain-forest parameter for AGB/carbon estimation for REDD+ and its MRV system by complimenting UAV imagery and TLS data.

The UAV images acquired with a strong overlap condition were processed to generate Digital Surface Model (DSM). The UAV-based Canopy Height Model (CHM) was developed by subtracting the LiDAR Digital Terrain Model (DTM) from the UAV-DSM. The upper canopy tree height derived from CHM generated from 3D image matching of UAV imagery compared with the tree height derived from ALS-CHM achieved an R^2 of 0.81 and RMSE of 2.1m (11%) and statistically, significance difference was observed. The UAV-based CHM overestimated the tree height by 1.26m when the overall mean tree height difference for 30 plots was calculated. The lower canopy tree height measured in the field when compared to tree height derived from TLS point clouds achieved an R^2 of 0.69 and RMSE of 1.4m (15%).The field measured height overestimated the lower canopy tree height by 0.30m when the overall mean tree height difference for 30 plots was calculated and no significance difference observed. The DBH derived from TLS point clouds when compared to field measured DBH achieved an R^2 of 0.986 and RMSE of 1.4cm (7%). The DBH derived from the TLS point clouds was underestimated by 0.28cm of the overall mean tree DBH difference for 30 plots and no statistical significance different was observed.

The derived AGB from the upper and lower canopies were combined. The accuracy of the forest AGB/carbon stock on plot base estimated by the developed method when compared to reference method achieved an R^2 of 0.98 and RMSE of 536.25Kg per plot (6.23%) for 30 plots. Also, a t-test shows no statistical significance difference between the AGB/carbon estimated by the two methods.

Based on the robust results, this study presented a novel method to address the need of the REDD+ and it's MRV mechanism to provide a cost-effective and accurate AGB/carbon assessment for a complex multi-layered tropical rain forest.

Keywords: TLS, UAV imagery, Photogrammetry, AGB, Carbon stock, REDD+ MRV mechanism

ACKNOWLEDGEMENTS

I would like to thank the Almighty God for all what he has done for me throughout this journey of my M.Sc., Glory and Honor to Him

I would like to express my appreciations to Joint Japan World Bank Graduate Scholarship Program (JJWGSP) who provided me a scholarship to pursue MSc degree at ITC (Faculty of Geo-information Science and Earth Observation-University of Twente). I am very grateful to my organization Mpingo Conservation and Development Initiative for giving me a leave to study in the Netherlands.

I am very grateful to express my sincere gratitude to my first supervisor Dr. Yousif Ali Hussin, for his continuous encouragement, fieldwork support, constructive feedback and comments from the very beginning till the completion of this research. It was a real opportunity and pleasure to work under his supervision. To my second supervisor, Drs. E. Henk Kloosterman, I am humbled to extend my sincere and deepest thanks for his supervision, productive responses, advises and intensive fieldwork support. Without the guidance of my supervisors', this research would hardly have come to fruition.

My sincere thanks go to Prof.Dr. A.D. Nelson for his constructive comments during the proposal and mid-term defenses. I am very much thankful to Drs. Raymond Nijmeijer, Course Director NRM, for his continuous support and feedback from the beginning of course to completion of research.

Special thanks go to the Faculty of Forestry, the University of Putra Malaysia (UPM) for their help and support throughout the field work period. Special thanks to Dr. Mohd Hasmadi for the hospitality and organization of the fieldwork. Also, special thanks go to Mr. Mohd Naeem Abdul Hafiz and his team of forest rangers who accompanied me daily and helped in the collection of the data. I am indebted to them for their commitment and putting in extra hours for me so that I could collect all the data needed to make this thesis successful.

I would like to extend genuine thanks to my fieldwork mates John Ruben, Mariam Adan, Muluken N. Bazezew and Solomon Ibn M. Many thanks to NRM classmates for fruitful time and joyfulness throughout the18 months of study. I am very appreciative to my great friends Benjamin Appiah, Krishna Lamsal, Grace Simon, Kelvin Kamde, Ghebregziabher Tumlisan, Paulina Asante, Samaher and the rest for their moral support and quality time spent together during the stay in the Netherlands.

I would like to recognize the support and assistance of Mr. Jasper Makala, Abby Willy, all MCDI co-workers and partner organizations for their support towards my professional career.

Finally, deepest appreciation goes to my lovely wife (Ney-Juve) for letting me come for my studies and manage to live without me during the period of study. To my parents, my brother and sisters for their tireless prayers and support throughout the 18 months of my MSc and the rest of my family members who always encourage me and wish for my success.

Yuvenal Pantaleo Mtui,
Enschede, the Netherlands
February 2017.

TABLE OF CONTENTS

LIST OF FIGURES

LIST OF TABLES

LIST OF EQUATIONS

LIST OF APPENDICES

LIST OF ACRONYMS

AGB	Aboveground Biomass
UAV	Unmanned Aerial Vehicle
SfM	Structure from Motion
CHM	Canopy Height Model
DBH	Diameter at Breast Height
DSM	Digital Surface Model
DTM	Digital Terrain Model
GPS	Global Positioning System
GCPs'	Ground control points
IPCC	Intergovernmental Panel on Climate Change
LiDAR	Light Detection and Ranging
MRVs'	Monitoring Reporting and Verifications
REDD	Reducing Emission from Deforestation and Forest Degradation
TLS	Terrestrial Laser Scanning
MSA	Multi Station Adjustment
RMSE	Root Mean Square Error
UNFCCC	United Nations Framework Convention on Climate Change
ALS	Airborne LiDAR System
UAV-DSM	Digital Surface Model generated from 3D image matching of UAV imagery
ALS-DTM	Digital Terrain Model generated from Airborne LiDAR point clouds
ALS-CHM	Airborne LiDAR System Canopy Height Model
UAV-CHM	Canopy height model developed using UAV-DSM and ALS-D

1. INTRODUCTION

1.1. Background

Tropical forests play a major role to sequester and store large amounts of carbon which act as a natural control of climate change and important global carbon budget (Gibbs et al., 2007). On the other hand, forest degradation and deforestation lead to carbon emissions, with global deforestation being among the drivers of the increase in atmospheric carbon dioxide (CO_2) (Mohren et al., 2012). The main carbon pools in tropical forest ecosystems are the living biomass of trees and undergrowth vegetation, the dead mass of litter, dead wood and soil organic matter. The carbon reserved in the aboveground living biomass of trees is typically the largest pool and the most instantly impacted by deforestation and degradation (Gibbs et al., 2007).

The United Nations Framework Convention on Climate Change (UNFCCC, 1997) report as cited by (Patenaude et al., 2004) direct human-induced emissions and removals of carbon dioxide to be reduced from Land Use Change and Forestry activities, which include deforestation, afforestation, and reforestation activities. In order to control the impact of climate change, the range of initiatives have been established, one of such program is Reducing Emissions from Deforestation and Degradation (REDD+) with its measuring reporting and verification (MRV) mechanism (Aikawa et al., 2012). REDD+ was designed to provide incentives to developing countries to reduce deforestation and forest degradation rates and support conservation measurements which reflect the value of the carbon sequestered and stored in trees (Angelsen et al., 2012).

The opportunity for tropical countries such as Malaysia to benefit from REDD+, required a cost-effective method for providing accurate and timely information to determine forest parameters for estimating AGB and carbon stock (Angelsen et al., 2012). Karna (2012) stated that the tree canopy height and diameter at breast height (DBH) or crown projection area are important forest inventory parameters for estimating Above Ground Biomass (AGB). The precise and unbiased biomass can be obtained through a destructive method which involves cutting trees, weighing, labor intensive as well as time- consuming and rather expensive. However, biomass estimation through a non-destructive method using an allometric equation which needs a direct measurement of DBH and Height as input parameters also can be expensive and time-consuming, therefore we need remote sensing technology. Remotely sensed data can be used as a cost-effective source of secondary information to improve the precision and timelines for generating the inputs forest parameters of an allometric equation for estimation of AGB and carbon stocks stored in the tropical rainforest (Mohren et al., 2012).

The remote sensing approach for AGB estimation varies from low optical resolution (MODIS, Landsat etc.) to high-resolution imagery (Geo-eye, Wordview-3 etc.), with horizontal forest structure information but cannot provide the vertical structure information (Bottcher et al., 2009). The airborne sensor such as LiDAR can provide vertical information for the derivation of canopy height model which can be combined with optical satellite sensor and improve AGB estimation (Zaki & Latif, 2016). There is some limitation associated with satellite-based research in multi-layered canopies of tropic rainforest for obtaining a real-time forest biomass and carbon stock estimation such as cloud cover, difficult to get suitable revisits time, low-resolution scenes, difficult to give accurate understory information and high cost per scene (Koh & Wich, 2012). Although, airborne sensors such as LiDAR is one of the most reliable tools used to provide the canopy height model (CHM) for estimating AGB with significance extent of accuracy in tropics.

However, the acquisition of airborne based data are often too expensive and a setback for regularly monitoring forest resources (Tesfai, 2015).

The emerging of Unmanned Aerial Vehicles (UAVs) which are lightweight, low-cost aircraft platforms operate from the ground that can address some of these operational issues. The UAVs offer a promising way for timely, cost-effective and approachable way for monitoring of natural resource at spatial and temporal resolutions that are appropriate to overcome the limitation related to satellite and airborne based research (Anderson & Gaston, 2013). There is a possibility to produce accurate canopy height model with UAV images by providing a close view of the upper canopy which assists in the retrieval of vertical forest structural parameters by subtracting with existing DTM see Figure 1-1 (Paneque-Galvez et al., 2014). Ota et al.,(2015) reveal that applying the Structure from Motion (SfM) approach can support the derivation of high spatial resolution 3D point cloud model from the photograph taken by UAV, similar to those derived from airborne LiDAR. Previous studies demonstrated the effectiveness of the SfM approach for topographic mapping and landslide monitoring. On the other hand, few studies evaluate the effectiveness of a canopy height model created by a SfM algorithm for derivation of tree height for upper canopy AGB estimation in the tropical countries.

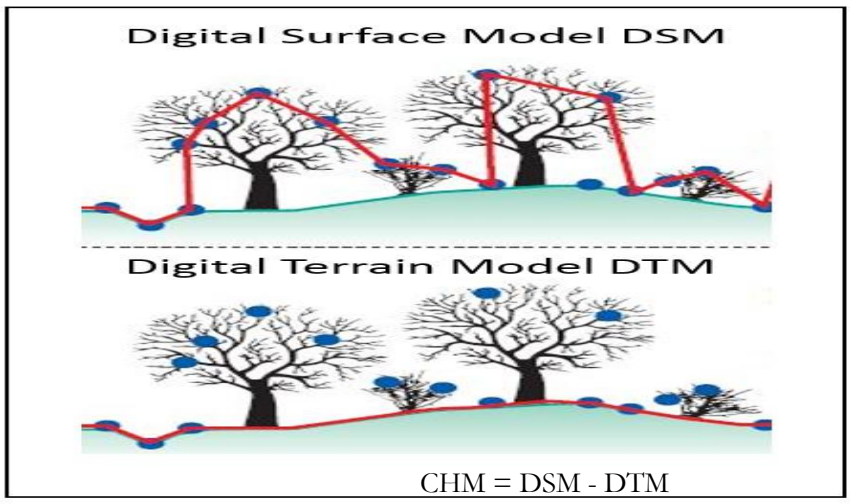

Source: http://www.charim.net/datamanagement/32

Figure 1-1: Graphs shown the difference between DSM and DTM

Direct measurements of understory vegetation parameters for lower canopy AGB estimation are time-consuming and destructive especially in the complex tropical forest where field work is labor intensive and tough. While TLS is a viable option for measuring the required information for understory vegetation assessment (Lawas, 2016, Madhibha, 2016, Kankare et al., 2013). It has been revealed by Srinivasan et al., (2014) that TLS can obtain accurate understory information and detailed vertical parameters for biomass estimation with better results when compared to airborne LiDAR and direct field measurements.

Therefore, alternative cost-effective approaches to obtain CHM for the upper canopy and access the understory vegetation details for accurate AGB estimation are required. This study aiming to assess AGB and carbon stock in Ayer-Hitam tropical rain-forest reserve in Malaysia using TLS data and upper canopy tree heights from canopy height model generated from UAV imagery.

1.2. Literature Review

1.2.1. Biomass and carbon stock in lowland Tropical rainforest

Tropical rainforests have large carbon stock and provide habitat for many of the world's species (Palace et al., 2016). This forest type is a structurally complex with different canopy layers namely understory canopy, continuous canopy and emergent canopy (Figure 1-4: Typical structure of tropical rain-forest) and therefore play a key role in climate change mitigation (Zaki & Latif, 2016). In a tropical forest ecosystem, the carbon pools are, the living biomass of trees, the understory vegetation, the deadwood, woody debris and soil organic matter. The AGB of the tree is the largest contributor to the forest carbon pool and it is impacted by deforestation and forest degradation(Vashum, et al., 2012).

1.2.2. Biomass and carbon stock

In this study, forest biomass is defined as the total amount of oven dried aboveground living organic matter expressed by tons per unit area and the carbon stock is 50% of AGB (Brown, 1997). Forest biomass and carbon stock play an important role in the global carbon cycle. Therefore, accurate quantification methods for AGB are required to support global initiatives such as REDD+. Previous studies showed that different inventory methods such as destructive sampling, allometric equations, and remote sensing have been practiced in the tropical rain forest for above-ground forest biomass estimation (Basuki et al., 2009).

1.2.3. Allometric equation

The commonly used method for estimating forest biomass is through an allometric equation. Various researchers have developed equations through destructive method to generalize the estimation of biomass per different forest type and tree species (Curtis, 2008). These equations are used to establishing a relationship of field measurements of tree parameters such as tree DBH, height, crown diameter, tree species and biomass through non-destructive method (Breu et al., 2012). According to Basuki et al., (2009), the use of site-specific allometric equation must be considered for accurate biomass estimation as they take into consideration the site effects. The allometric equation developed by Chave et al., (2014) is a very good example for such equation to assess AGB.

Equation 1-1: Allometric equation (Above Ground Biomass)

$$AGB_{est} = 0.0673 \times (\rho D^2 H)^{0.976}$$ …… Equation 1 source:(Chave et al., 2014)

Where AGBest is estimated above ground biomass in kilograms (Kg), D is diameter at breast height in centimeters, H is tree height in meters (M) and ϱ is wood specific gravity in gram per cubic centimeters.

1.2.4. The TLS in Forest Application

Terrestrial laser scanning (TLS) is an instrument acquires accurate dense 3D point clouds of the surrounding environment using laser and scanning system (Zheng et al., 2016). Reflected light pulses are detected by the system and time of flight is recorded. Based on some pre-determined algorithm the distance from the target object based on the time recorded and speed of light are calculated to generate useful information about the object (Newnham et al., 2015). This technology allows acquisition of forest structure parameters in the form of the 3D point cloud, which can be processed and provide DBH, height and location of trees which are crucial parameters for forest biomass and carbon stock estimation (Wezyk et al., 2007).

Figure 1-2: RIEGL VZ-400 without Camera and with Camera

The TLS RIEGL VZ-400 (Figure 1-2) is a very good example of TLS which is a waveform recording instrument with fine scan resolution. A study carried out by Newnham et al., (2015) revealed that RIEGL VZ400 instrument can provide accurate forest structural information for forest biomass estimation.

1.2.5. The UAV in forest application

The Unmanned Aerial Vehicles (UAV) well-known as Drones were initially developed for military purposes, but recently find their way into civilian and natural resources applications such as forest monitoring, surveillance, mapping and three-dimensional (3D) modeling (Ritter, 2014). According to Turner et al., (2012) there are two categories of UAV system, fixed wing and multi-rotors or copters (Figure 1-3). They have a different performance based on payload, flight time and stability in image acquisition. A fixed wing UAV travels faster and cover a larger area, thus to maintain a proper image overlap. The fixed wing UAV needs to fly higher to ensure that the footprint and the overlap are larger. On the other hand, Multi-rotors (helicopter) UAV can capture images at almost any overlap, possible to fly very low and capture extremely high-resolution data if required.

Figure 1-3: The two categories of UAV system and sample of UAV image

UAV applications in forest monitoring have a number of advantages over established remote-sensing methods. They can provide extremely high spatial and temporal resolution thus allows the identification of very small object in details, and images are infrequently affected by cloud because of low flying altitudes. Flight missions can be timed to avoid any limitation, and they are very cost-effective to boost forest inventories in tropical countries, which is essential for REDD+ MRV systems (Getzin et al., 2012).
The study carried out by Ritter, (2014) revealed that, the advancement in digital photogrammetric processing using automated methods such as SfM (Structure from Motion) has proven that the image taken by UAV can be processed and generate 3D points cloud with spatial information which can be used to generate Digital Surface Model (DSM) where different methods can be utilized and provide accurate canopy height model (CHM).

1.2.6. Integration of TLS and UAV in forest Application

UAVs have received rising attention in forest application, as a result of the effectiveness of SfM approach for reconstruction of DTM and DSM which can be used to produce detailed forest resource data such as tree canopy height model and orthophoto. Hence tree height estimation for tree biomass and carbon estimation (Aicardi et al., 2016). In this system, the height of the tree and other parameters can be obtained and the UAV imagery can be acquired regularly at low cost compare to Airborne LiDAR and reduces the field survey cost significantly (Uramoto et al., 2012). On the other hand, retrieving DBH from the aerial images is the least challenge. Liang et al., (2016) revealed that TLS techniques have gained scientific and operational interest in natural resource management, especially in forest applications due to its ability to acquire detailed forest structure parameters from the ground view. The study carried out by Aicardi et al., (2016) suggested the two methods provided both ground-based and aerial views forest structure information and supplemented each other to overcome the limitation associated with each method. The limitation associated with TLS technique is lacking upper canopy information from the ground view due to foliage coverage which was resolved by aerial imagery from UAV datasets while the limitation of aerial photogrammetric from UAV to capture the ground information was supplemented by TLS by providing accurate tree trunk information and facilitate forest structure assessment and monitoring.

1.2.7. Validation of forest parameters

ALS Canopy Height Model

Measuring tree height based on the traditional field survey in tropical rain-forest sometimes is unreliable based on its multi-layered forest structure with dense understory and wide canopies which can block the view to the top of the upper canopy trees for accurate measurement (Hunter et al., 2013). A study carried out by Sadadi, (2016) revealed that tree height measured by ALS can be used as a standard as it proved to yield more accurate upper canopy height data than field-based measurement. Therefore, this study relied on the tree height from the existing CHM generated from ALS to validate the upper canopy tree height derived from CHM developed from UAV imagery.

TLS derived tree height

Based on the experiment conducted in ITC prior to field work shows that TLS measurement are very accurate and tree height measured with a handheld instrument device are unreliable, particularly in a situation with a complex forest structure. The Laser handheld instrument shows a variation when tested on the secondary forest. Therefore, the height derived from the TLS point cloud can be considered as a reference tree height for the lower canopy.

1.3. Problem Statement

To mitigate climate change the Reducing Emissions from Deforestation and Forest Degradation in Developing Countries (REDD+) and its MRV mechanism under the UNFCCC was initiated. MRVs is calling for the use of the cost-effective method for providing accurate and timely information of the forest parameters across the complex multi-layered lowland tropical rain forest for estimation of forest biomass and carbon stock which is essential to boost the opportunity for tropical countries to benefit from REDD+(FAO, 2010).

The tropical rainforest is characterized by three layers of trees (Figure 1-4) which are emergent trees, continuous canopy (main stratum) and understory canopy (Nurul-Shida et al., 2014). The accurate and cost-effective method for assessing the AGB by taking into consideration trees in all canopy layers of the tropical forest complex structure is required. Vashum et al., (2012) stated that the tree canopy height and DBH are common forest parameters for developing allometric equations for estimating AGB. Measuring tree height and DBH by field surveying are time consuming, limited to inaccessible areas and rather expensive.

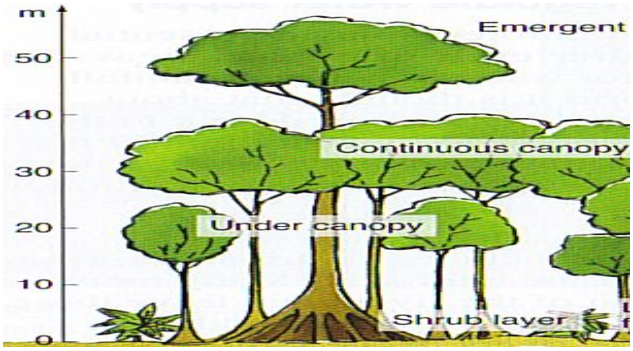

(Source: http://www.acegeography.com)

Figure 1-4: Typical structure of tropical rain-forest

The current rapidly growing of remote sensing technology in which various methodologies has been developed using high-resolution images in combination with Radar or LiDAR data and complimented by Terrestrial Laser Scanner to derive the forest structure parameters across different canopy layers. However, some of the data set such as airborne LiDAR and Radar are quite expensive to acquire for regular monitoring purpose and not always available.

The emerging of Unmanned Aerial Vehicles (UAVs') which are lightweight, low-cost aircraft platforms operate from the ground, offer a promising way for timely, cost-effective and approachable way for monitoring natural resource at high spatial and temporal resolutions that are appropriate to overcome the limitation related to satellite and airborne based research (Anderson & Gaston, 2013). Previous studies have shown that using the UAV image through automatic image matching technique a photometric digital canopy surface model (DSM) can be generated (Figure 1-5). Once the DTM is available it can remain constant for a long time while DSM needs to be up-to-date and accurate to generate accurate forest canopy height model that would assist in the retrieval of tree canopy height (Lisein et al., 2013). The limitations associated with this method compared to LiDAR is that they cover a small area and sometimes impossible to acquire the lower canopy information from the aerial view for assessing understory trees as well as DTM. Therefore, the CHM is applicable for upper canopy biomass estimation only. However, UAV imagery can be acquired regularly at low-cost compared to Airborne LiDAR and reduce the field survey cost significantly which give it value approachable way to replace LiDAR on regular monitoring purpose (Uramoto et al., 2012).

Source: (Lisein, 2012)

Figure 1-5: Schema for canopy height model

Terrestrial laser scanners (TLS) is a very useful and robust method for measuring forest structure through non-destructive technique particularly in a tropical forest, where the direct method is often tough, labor intensive, prone to human measurement error and expensive (Palace et al., 2016). TLS has proven to acquire three-dimensional data of standing trees from the ground view accurately and rapidly through a non-destructive method, which has made this technology more widely used in studying forest structure (Madhibha, 2016, Lawas, 2016). Srinivasan et al., (2014) revealed that TLS can provide accurate understory information and detailed forest vertical structure measurements as DBH, tree height and tree location for better estimation of lower canopy biomass when compared to other techniques such as airborne LiDAR and field measurements. The limitation associated with this method compared to airborne LiDAR is that sometimes underestimating the upper canopy height due to foliage coverage and the distance of a device to the upper canopy which hinder the TLS pulse to access the upper canopy from the ground view. Therefore TLS can accurately assess DBH and height of lower canopy trees and the DBH of upper canopy trees while UAV 3D image matching data can assess the height of upper canopy trees.

This study is therefore intended to assess the performance of combining the information on upper canopy tree heights from canopy height model generated from 3D image matching of UAV imagery and TLS data which can estimate the lower canopy DBH and height and upper canopy DBH and consequently estimate biomass and carbon stock in tropical rain-forest. This offers the potential to establish an accurate and cost-effective approach that can be used for estimating AGB and significantly contribute to the REDD+ and its MRVs' mechanism.

1.4. Research objectives

1.4.1. The main Objective

To test the performance of integrating Terrestrial Laser Scanner data and tree height from CHM generated from 3D image matching of UAV imagery for plot-based upper and lower canopies above ground biomass and carbon stock estimation in Ayer-Hitam tropical forest.

1.4.2. Specific Objective

- To assess tree height derived from a CHM based on 3D image matching of UAV imagery for upper canopy trees compared to ALS Canopy Height Model.
- To assess lower canopy tree height measured in the field compared to tree height derived from TLS data.
- To assess the accuracy of the DBH measured by TLS compared to DBH measured in the field (manual).

- To estimate plot-based AGB and carbon stock and assess its accuracy in relation to AGB and carbon compared to AGB (Field DBH + TLS lower canopy height + ALS upper canopy height)

1.5. Research question

- How accurate is the upper canopy tree height derived from CHM developed using 3D image matching of UAV imagery compared to ALS Canopy Height Model?

- How accurate is the lower canopy tree height measured in the field compared to tree height derived from TLS data?

- How accurate is the DBH derived from TLS data compared to field measurement?

- How accurate is forest AGB/carbon stock on plot base estimated by the developed method (TLS DBH+TLS lower canopy height + upper canopy UAV height) compared to the reference method (Field DBH + TLS lower canopy height + ALS upper canopy height)?

1.6. Hypotheses or anticipated results

- H_0: The accuracy of the tree height developed from 3D image matching of UAV imagery is < 80% compared to the height from ALS Canopy Height Model.
- H_1: The accuracy of the tree height developed from 3D image matching of UAV imagery is ≥80% compared to the height from ALS Canopy Height Model.

- H_0: The accuracy of the tree height from field measurement for the lower canopy is<80% compared to lower canopy tree height derived from TLS data.
- H_1: The accuracy of the tree height from field measurement for the lower canopy is ≥80% compared to lower canopy tree height derived from TLS.

- H_0: The accuracy of the DBH derived from TLS data for AGB estimation is <90% compared to field measurement.
- H_1: The accuracy of the DBH derived from TLS data for AGB estimation is ≥90 compared to field measurement.

- H_0: The accuracy of AGB estimated on a plot base from TLS data and CHM from 3D image matching of UAV imagery <90% compared the reference method (Field DBH + TLS lower canopy height + ALS upper canopy height).
- H_1: The accuracy of AGB estimated on plot base from TLS data and CHM from 3D image matching of UAV imagery ≥90% compared to the reference method (Field DBH + TLS lower canopy height + ALS upper canopy height).

2. STUDY AREA AND MATERIALS

2.1. Study area

2.1.1. Geographical Location

This study was conducted in Ayer Hitam Forest Reserve (AHFR). It is a tropical rainforest covers an area of 1,248 hectares and located in Puchong, the state of Selangor, Peninsular Malaysia (03° 01' N, 101° 39' E), and approximately 45 kilometres from the city of Kuala Lumpur (Hasmadi et al., 2008). AHFR is surrounded by residential and other economic development activities which isolate the forest from another forest (Figure 2-1). The study area was selected based on the logistic support of the University of Putra Malaysia who managing this forest for the purpose of teaching, research and extension activities since October 1996 (Lepun et al., 2007). The logistical requirements include the local knowledge for navigation, tree species identification, and availability of Airborne LiDAR data.

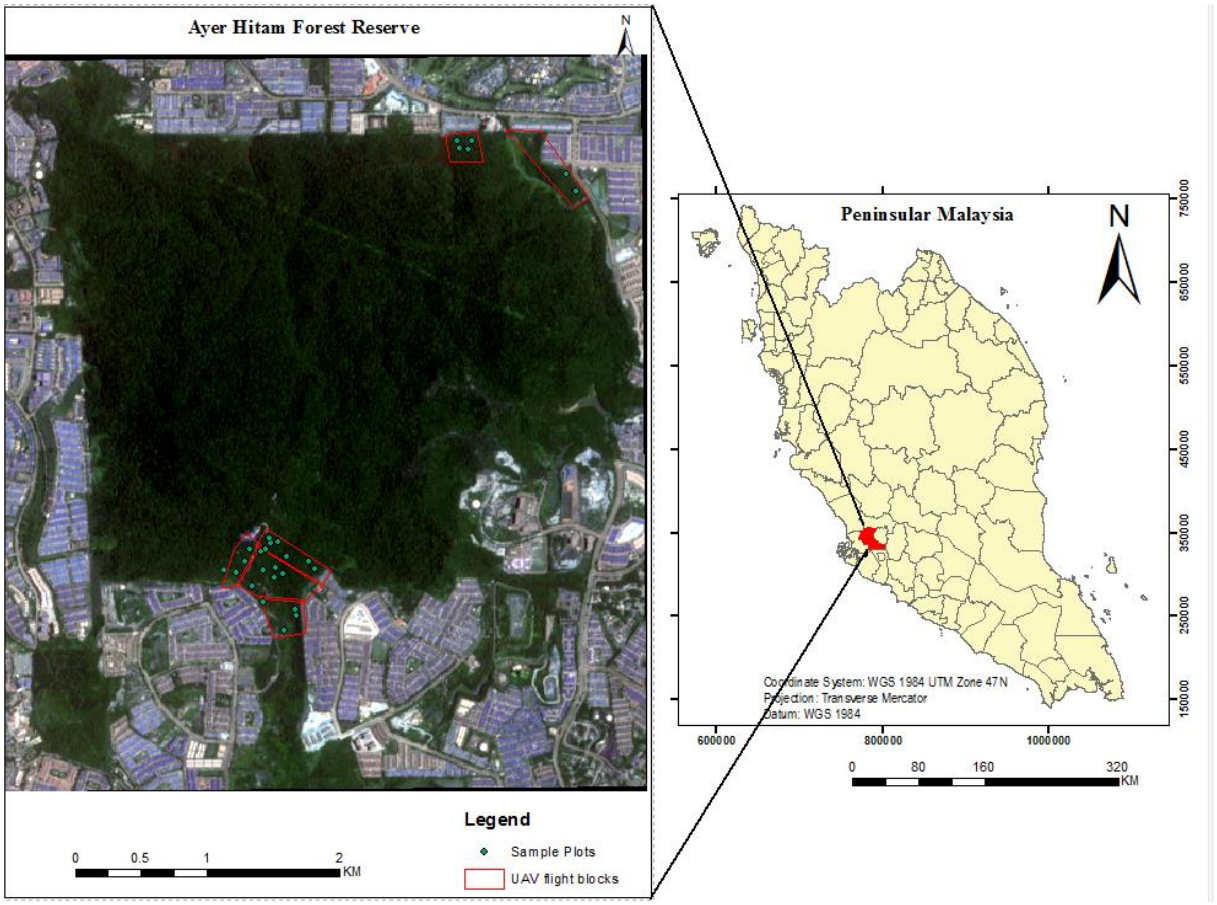

Figure 2-1: Map shown the study area of Ayer Hitam Forest Reserve

2.1.2. Climate and Topography

The Ayer Hitam Forest Reserve is tropical rain forest with an average temperature of 27.8°C where a maximum and minimum temperature is 32.6°C and 24.6°C respectively while the relative moisture is 83% and average annual rainfall is 2178mm (Lawas, 2016, Lepun et al., 2007). The landscape of the study area is undulating with several different topographical characteristics such as hillsides, ridge, and valley. The terrain is moderately steep with a slope of up to 34° and elevation ranges from 15-233m(Hasmadi et al., 2008).

2.1.3. Vegetation

The Ayer Hitam Forest Reserve is classified as logged-over lowland mixed dipterocarp tropical forest with a dense, multi-layered vegetation structure which is still regenerating with 430 species in 203 genera and 72 families found in this forest (Hasmadi et al., 2008). The forest is dominated by a high density of small and medium size trees with the forest floor covered by seedlings and saplings as well as herbs, climbers, creepers, palms and ferns (Nurul-Shida et al., 2014).

2.2. Materials

2.2.1. Field instruments and Equipment

Different field instruments and equipment were used in the field to measure forest parameters in the field for AGB/carbon estimation. The field instruments listed below (Table 2-1) was used in this study for navigation to the sample plots, measuring of forest parameters.

Table 2-1: List of instrument used in field for data collection

Instruments/equipment	Application
Leica DISTO D5	Tree height measurement
Diameter tape (5 meters)	DBH measurement
Measuring tape (30 meters)	Plot setting
Satellite image	Sample plot identification
Garmin GPS	Navigation and positioning
RIEGL VZ-400- TLS	Tree Scanning within plots
Sunto Clinometers	Slope measurement
Tablet	Navigation

2.2.1. Software and Tools

The list of different software packages used for processing and analysis of datasets are given in Table 2-2 below

Table 2-2: List of software packages used in this research

Software and tools	Purposes/Use
ERDAS IMAGINE 2015	Image Processing
MAPC2MA C64	Conversion of images into mobile device format
RiSCAN PRO	TLS data processing
ArcGIS 10.4.1	GIS tasks, Digital Elevation Model analysis
Agisoft Photoscan Professional	UAV image processing
LaStools	Conversion of LiDAR DTM format
Mendeley Desktop	Supporting proper references
MS Office 2013 (Excel)	Statistical analysis
MS Office 2013 (Word)	Reports and Thesis writing

3. RESEARCH METHODS

The methods used in this study comprises of three (3) parts:

1. Field measurements of lower canopy tree height using Leica DISTO D5 and DBH using diameter tape
2. Use of TLS scanner for the generation of a 3D point cloud of the sample plot
3. UAV image acquisition for the derivation of tree height of the upper canopy for biomass and carbon estimation.

The workflow is illustrated (Figure 3-1) in the flowchart below Flowchart

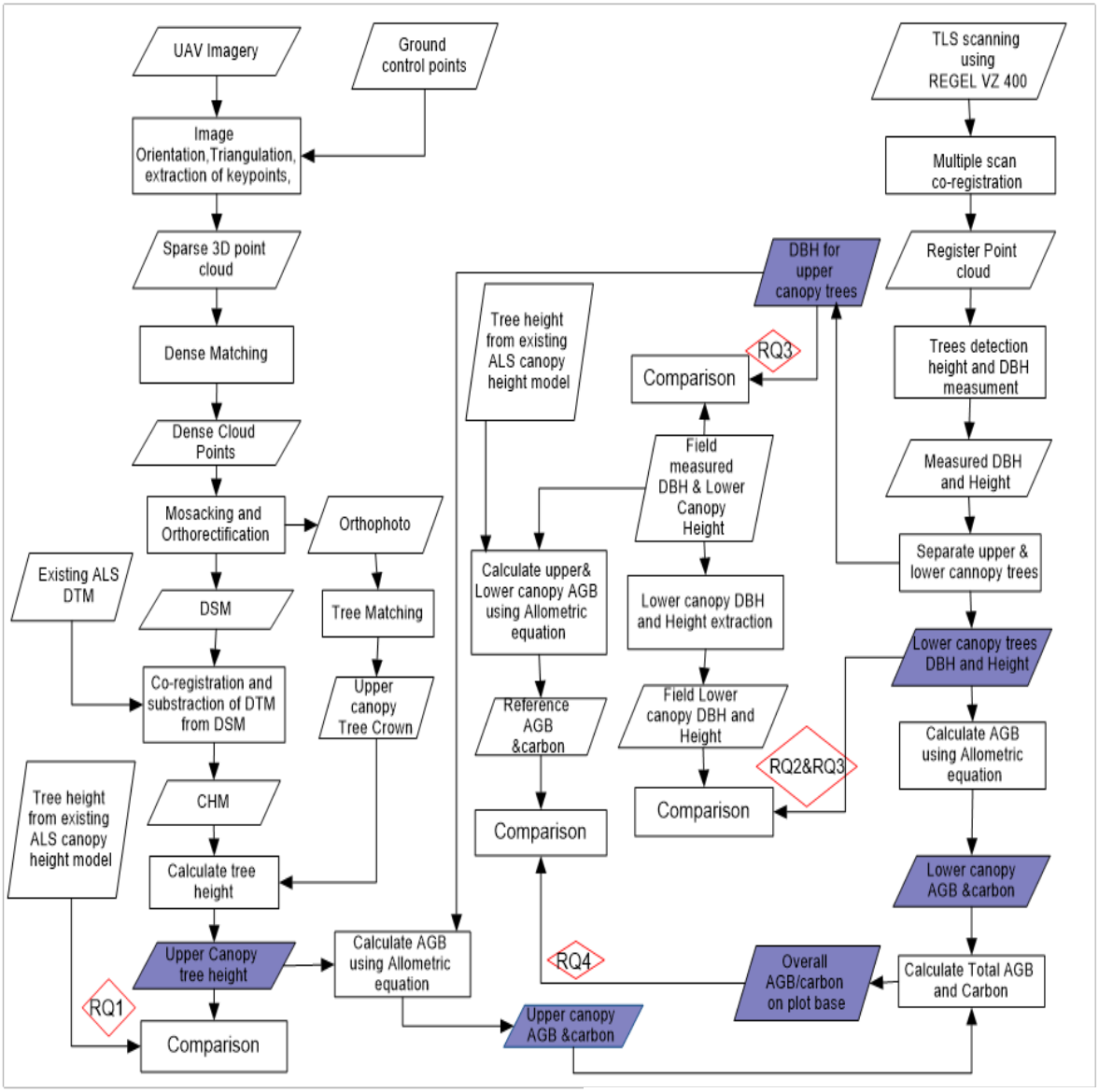

Figure 3-1: Flowchart of the research method.

RQ: Research Questions

3.1. Plot size

Circular sample plots of 500 m² with a 12.62 m radius on flat terrain were used for the measurement of the forest parameters. The circular plots are easy to establish and less exposed to errors in the plot area than square plots. Since the length of the boundary of the circular plot is smaller than in square plot, there may be few trees located on the edge (Lackmann, 2011).

3.2. Sampling design

A purposive sampling method was used in this study. The plot selection aimed at covering the variation across the dense, complex forest vegetation structure and due to the weight of the TLS (23 kg), taking accessibility (slope steepness, the penetrability of the undergrowth and distance to the road) into account (Figure 3-2). This sampling design is non-probability method where the sample plots choice is based on the researcher judgment.

Figure 3-2: Sample plot on steep slope in Ayer Hitam Forest before and after clearing the undergrowth

The plots were selected in the areas flown by the UAV (Figure 3-3) with a distance of more than 50 meters apart. The coordinates of the center of the plot was recorded (WGS 1984) with handheld GPS (Garmin).
A total of 27 sample plots were surveyed and 3 sample plots surveyed in 2015 which fall within the UAV flight areas were included, making the overall number of sample plots for this study to be 30.

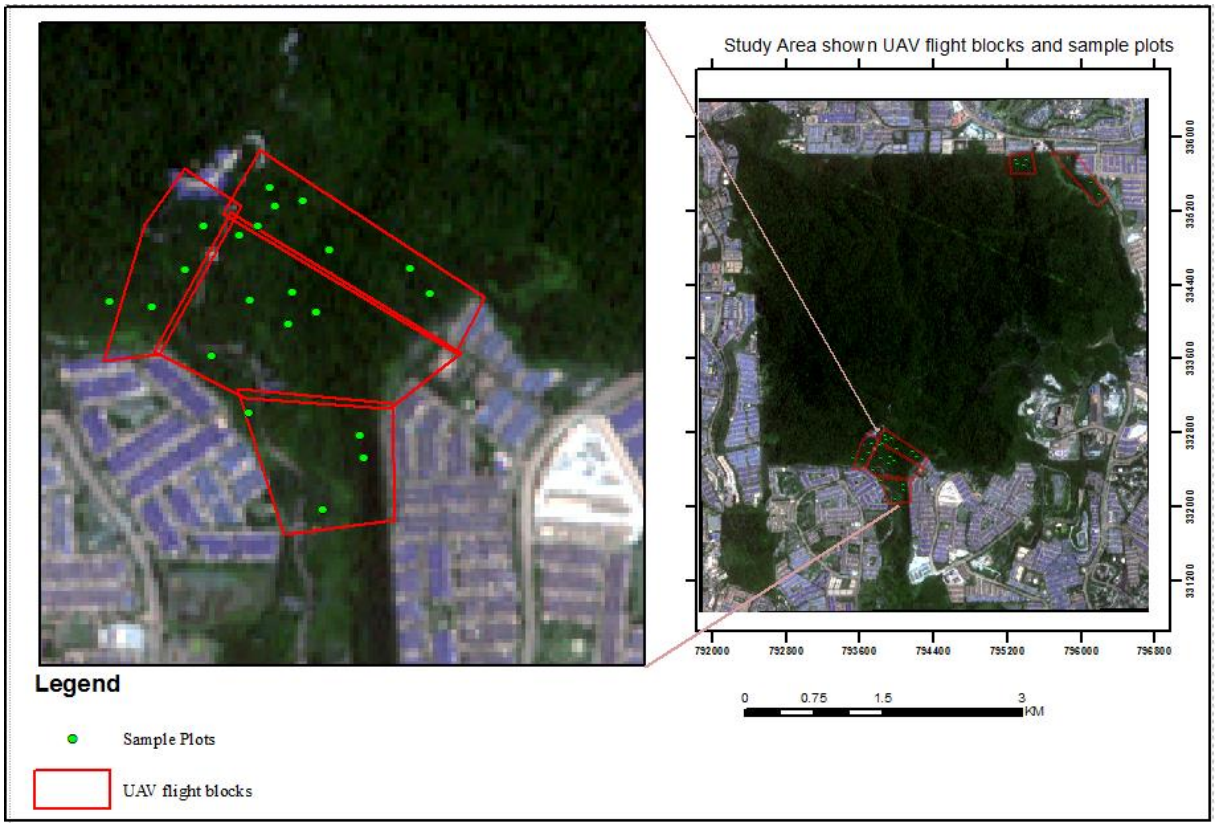

Figure 3-3: Study area map shows the part of UAV flight blocks and sample plots

3.3. Field data collection

3.3.1. Biometric measurement

This involved the measuring of tree height, crown diameter, Diameter at Breast Height (DBH) for the trees with DBH equal or greater than 10cm and identification of tree species. The DBH was measured using diameter tape at 1.3m above ground. Trees with DBH less than 10 centimeters were excluded since they contribute very little on the total forest AGB (Brown, 2002). The lower canopy tree height was measured in the field using Leica DISTO D5 and extracted from the 3D point cloud from TLS scan (see section 3.5.2). The tree crown diameter was measured using a measuring tape with the purpose of supporting the tree matching process for upper canopy tree identification from the UAV ortho-mosaic and CHM. From all trees included in the sample, the scientific name was determined by a local botanist. This information is necessary to establish the tree species wood density as an input parameter of the allometric equation for estimation of AGB and carbon stock. The measured parameters were recorded on the data collection sheet (Appendix 7).

3.3.2. Data collection using the TLS

Multiple scans approach with four (4) scan positions was used for every circular sample plot (Figure 3-5) in this study. The setup of multiple scans for the acquisition of the TLS scans described in the following subsections:-

Plot Preparation for Scanning

After the plot was cleared from undergrowth and palm trees, the plot center was located at least one meter away from the trunk of the tree to ensure the TLS clear view of trees within the plot. The areas with a slope greater than 5% a slope correction were applied based on the slope correction factor using the slope

correction table (Appendix 6). The undergrowth was cleared for a clear view for TLS of the tree trunk and tree crown. Trees with a DBH greater or equal to 10 cm were marked with laminated tags (Figure 3-4).

Setting the Tie points

The reference retro-reflectors (used as tie points) set up was important for accurately co-registers and geo-referencing the four separate scans of the plot. Both cylindrical and circular retro-reflectors were used in this study. A 12-15 cylindrical retro-reflectors were positioned on top of the stick for a clear view from all scan positions and 4-6 circular retro-reflectors were pinned on the tree stem facing the plot centre in such a way that they could be visible from the centre scan position and at least one was visible by the three outer scan positions (Figure 3-4).

Figure 3-4: Shown the tagged trees, overlaid cloud points, set up of cylindrical and circular retro-reflectors

TLS scanning positions

The first scan position was at the center of the plot and the other three were located outside the plot just 15m from the center of the plot (Figure 3-5) in an angle of 120 degrees determined by TLS tripods (Wezyk et al., 2007). The multiple scan approach can reduce the problem of occlusion that caused by tree stem, branches or other understory vegetation near the scanner location and provide a more detailed 3D representation of trees in the plot for more accurate extraction and measurement of tree parameters (Kankare, 2015).

Setting the TLS and Scanning

The setup of the TLS involved manually leveling of the instrument by adjusting the tripod legs until the scanner was equal or close to one degree of the level (UNAVOC, 2013). The TLS was set to collect data in full wavelength with panorama 60 resolution and 13 digital images, collected by the digital camera, that were used to colour the point clouds. Also, the system was set to run fine search and registration of the tie points.

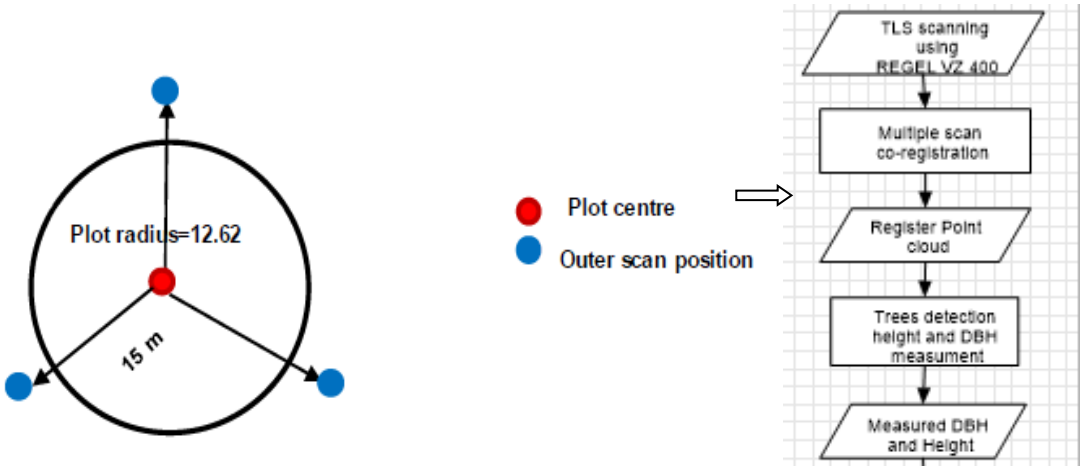

Figure 3-5: Circular plot for TLS multi-scanning and data processing workflow

(Source:(Lawas, 2016)

3.3.3. Data collection using UAV

The aerial image acquisition using UAV, commonly known as a drone involved two steps:

1. Choice of the UAV system
2. Data acquisition strategy

Choice of the UAV system

There are two categories of UAV systems, fixed-wing and multi-rotors UAV systems. Each system has a different performance in terms of flight time and stability in data acquisition. In this study, the aerial image acquisition was performed using multi-rotary UAV (DJI Phantom 4), which is suitable in the tropical forest where vertical flight is required. Although they cover a smaller area compared to fixed wing UAV systems which cover a wider area but cannot take off and land vertically (Aicardi et al., 2016).

UAV Data Acquisition Strategy

Data acquisition strategy involves the mission planning, GCP's allocation followed by the actual flight and data acquisition.

Mission Planning

The mission planning software (PIX4D Capture) was used to define the parameters (Table 3-1) to guide the UAV to perform the flight on the six (6) blocks where the sample plots were located. The flight height depended on the terrain of the flight block and the starting point was located in the area with high elevation to avoid crushing of the UAV on the tall trees in the hills.

Table 3-1: Technical parameters to guide UAV data acquisition

UAV Speed	9m/s
Front overlap	80%
Side overlap	60%
Flying height	80 and 90 meters
Resolution	4000x3000

GCP's allocation

The Ground control points (GCP's) were allocated to assist spatial referencing of the 3D model generated from the images. These points were pre-marked on the ground in a position that can be viewed by the UAV and can clearly be seen in the images (Figure 3-6).The GCP's locations were measured with high accuracy using Differential GPS.

Data acquisition

Based on the defined parameters during mission planning (position, altitude and flight line) the UAV recorded the digital images (Figure 3-6). All the images were stored on the UAV memory card and the qualities of the images were assessed after every flight.

Figure 3-6: The UAV flying (left) and GCP's maker (right)

3.4. Data Processing

3.4.1. Biometric data

The collected field data was entered in Excel sheet ready for analysis. The field data comprised of a plot number, tree number, location, DBH, Height, crown diameter, the scientific name of tree species and wood density. Based on the tree height measured in the field and derived from TLS data, the height of the tree that was not fully captured by the TLS was considered as upper canopy trees. Next to this, a threshold of 12 m was a set up to separate the lower canopy from upper canopy trees for the multilayer forest plots while 8 m threshold was used to separate the lower canopy from upper canopy for the less complex forest plots (plot 1, 26, 27 and 28). The threshold was selected based on the minimum tree height observed on the orthophoto and ALS-CHM.

3.4.2. Processing TLS data

Processing the TLS points cloud involves several steps as detailed in the following subsections:

Registration

Registration of multiple scans is the process of merging the separate scans into single 3D point clouds by geometrical transformation, based on the tie points placed in the plot and visible in all the four scans (Bienert et al.,2006). For this study, registration using the corresponding tie points was employed where the RiSCAN PRO v2.1 software was used to register the three outer scans to the center scan position which was the home scan and presents the project coordinate system. This process was followed by Multi-station Adjustment which involved two steps namely data preparation and running the Multi-station adjustment process. The Multi-station adjustment is the process which iteratively adjusts the position and orientation of the scans position to minimize the alignment error of the scan data which may be the result of unstable tie points set up or measurement errors (UNAVOC, 2013).

Extraction of Plot

The georeferenced and registered multiple scan position point clouds covered a larger area than the actual plot size, therefore, the point clouds within the plot range base on the recorded plot radius after slope correction were filtered using the range tool of RiSCAN PRO software. All the point clouds within the plot radius were extracted and saved as a poly data file for individual tree detection and extraction for DBH and height measurement.

Extraction of individual Trees

The tree extraction was carried out using the RiSCAN PRO software. The extracted plot was displayed on liner true colour to enhance visualization of the tree tags for individual tree identification and separation. The selection tools were used to select the trees based on their shapes then clipped out and saved individually as polydata followed by manual removal of the undergrowth, branches from other trees to capture properly the full tree. It was challenging to identify tree tag numbers for some trees but it was resolved by overlay the tree point clouds with the images taken by the TLS mounted a digital camera and the tree numbers were identified (Figure 3-4).

Extraction of Tree Parameters

The tree DBH and height were measured for all extracted individual trees. The details on how the trees parameters were measured using the RiSCAN PRO are described in the following subsections.

Measurement of Tree DBH

The DBH for each of the extracted individual tree was manually measured using the distance tool in the RiSCAN PRO software. The DBH was measured as the horizontal distance at 1.3m above the base of the tree stem (Figure 3-7). The tree DBH was recorded on the Microsoft Excel sheet for further analysis.

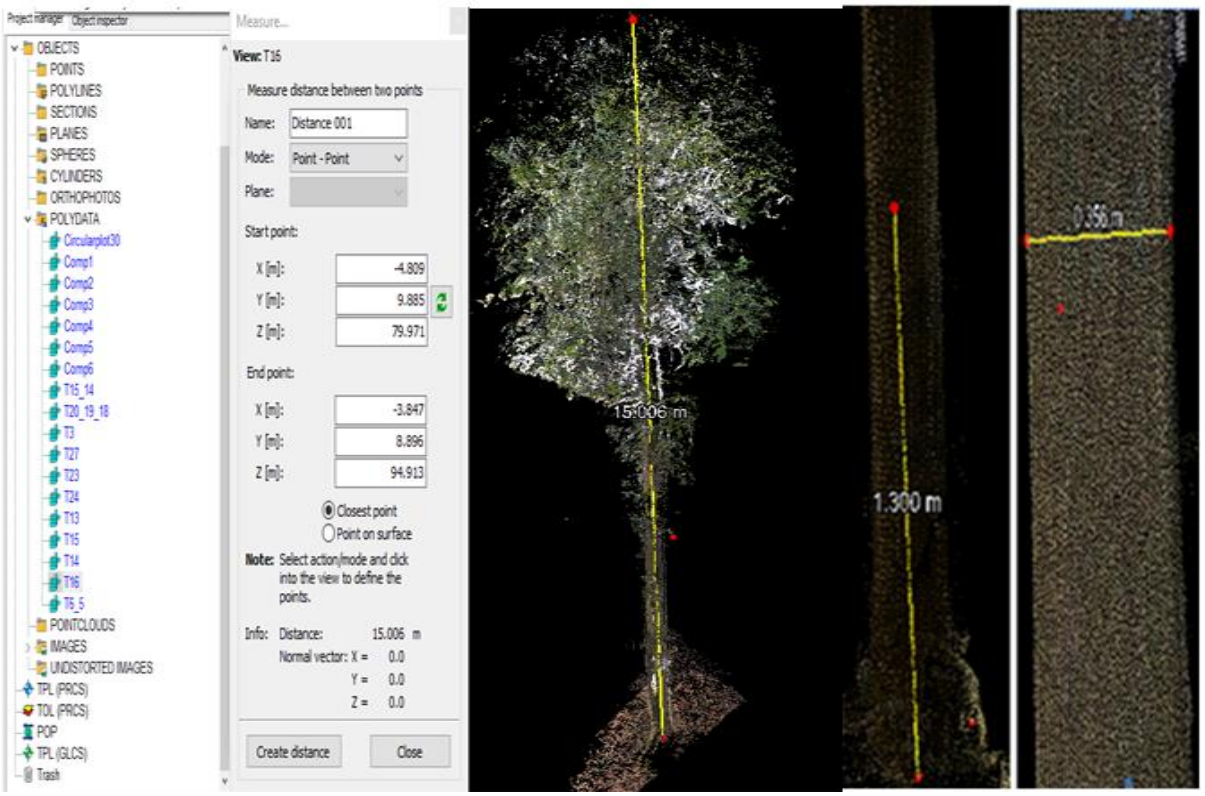

Figure 3-7: DBH and Tree height measurement of extracted individual trees

Measurement of Tree Height

The tree height measurement was also carried out for each of the extracted individual trees using the distance tool (point to point) in RiSCAN PRO software. The lowest point on the ground and the highest point of each tree were located and the distance between the ground and highest point was measured along the vertical axis to obtain the tree height (Figure 3-7). The tree height was recorded on the Microsoft Excel sheet for further analysis.

3.4.3. UAV Image Processing

The photogrammetric software Agisoft® Photoscan Professional trial licensed version was used to generate the DSM and Ortho-mosaic from the UAV images base on the automatic image matching method SfM (Structure from Motion). The photogrammetric workflow from Lisein, (2012) was adopted in this study which involves 7 steps:

1. Image Orientation and alignment process and subsequently the optimization of camera alignment using the GCPs'.
2. Dense Image Matching (DIM) aimed to compute a depth value for each corresponding pixel of images and result to the dense point cloud.
3. Orthorectified mosaicking process where the DSM and Orthophoto are interpolated from dense cloud point.
4. Build and export ortho-mosaic and UAV-DSM.
5. Generation of High-resolution CHM by subtracting LiDAR-DTM from UAV-DSM.
6. Tree height matching based on the tree location data collected in the field with the support of orthophoto followed by height calculation from both UAV-CHM and ALS-CHM.
7. Comparison of the tree heights extracted from the UAV-CHM with the tree height from ALS-CHM.

These details are more described in the following subsections:

Image orientation and Alignment

The images were uploaded to the software (Agisoft Photoscan) and the quality was assessed using the software automatic image quality estimation function. The maximum value for high-quality images is 1 unit and the values of the images acquired ranges between 0.8-0.9 units which indicated a good quality. The software recommends that images with a quality value less than 0.5 units be excluded from further processing, provided that the remaining images cover the whole study area (Agisoft, 2014). The medium and high accuracy setting were used to obtain accurate camera position estimates, followed by photo-alignment where the algorithm searches for common matching points between overlapping images and adjust a camera position for each photo and constructs sparse point clouds model (Leon et al., 2015). The output of this process is computed camera positions and a sparse point cloud.

Marker Placement (GCPs')

Photoscan software supports two approaches of marker placement, manual marker placement and guided marker placement. The manual approach was applied in this study where the ground control points were manually identified and indicated on each photo were the marker was visible. A minimum of four GCP's was used on each block to adjust the image alignment and georeferenced the generated model allowing for more precise geo-referencing.

Optimization of camera alignment

Photoscan calculates internal and external camera orientation parameters during image alignment stage, using image data alone. The accuracy of the final estimates depends on many factors, such as overlap between the neighboring photos, as well as on the shape of the object surface. These errors can lead to non-linear deformations of the final model (Agisoft, 2014). Generally, it is reasonable to run optimization procedure based on GCPs' data only to minimize the deformations, for the reason that the GCPs' coordinates are measured with significantly higher accuracy (using Differential GPS station) compared to the UAV GPS data that indicates camera positions (Leon et al., 2015). The optimization involved two steps, first the sparse point clouds was edited manually by removing noticeable outliers and misallocated points and secondly the GCPs' were used to run the optimization process. The GCPs' locations measured with high accuracy by differential GPS were certain to give more precise optimization results.

Photoscan software assumes that the manually entered GCPs' coordinates are exactly known, and will exclude the coordinates taken by the UAV and the geo-referencing accuracy was improved compared to accuracy achieved using the UAV GPS data (Agisoft, 2014). It is recommended to perform optimization if the final model is to be used for any kind of measurements.

Dense point cloud generation

The Photoscan built dense cloud points based on the estimated camera positions and the sparse cloud. The high accuracy point clouds were generated based on the estimated camera positions where the software computes a depth information for each camera to be combined into a single dense point cloud.

Digital Surface Model (DSM) generation

A DSM represents a surface model as a regular grid of height values. Within Photoscan a DSM can be generated from the dense point cloud, a sparse point cloud or a mesh. In this study, the DSM was generated based on the dense point cloud where the most accurate results can be obtained and exported using pixel resolution of 1 meter to match the resolution of the existing LiDAR-DTM.

Building Orthomosaic

The ortho-mosaic generation in Photoscan was undertaken by calculating a texture atlas for the model which was used to create the orthophoto mosaic. Ortho-mosaic export is normally used for generation of high-resolution imagery based on the source photos and reconstructed model.

Canopy Height Model Generation

The UAV-CHM was generated by subtracting the LiDAR-DTM from the UAV-DSM using Arc GIS Raster calculator tool and both with the same pixel size resolution of 1meter. The LiDAR DTM performs better than the UAV-DTM as LiDAR has the ability to capture multiple returns and penetrate to reach the ground. Hence accuracy improvement of measured parameters is anticipated. Also, the DTM can be constant for a long time while DSM needs to be up-to-date and accurate.

Validation of the UAV CHM

The tree's heights extracted from the UAV-CHM were compared with tree height extracted from the existing LiDAR-CHM using regression analysis and t-test. The performance was presented in terms of the model fit coefficient (R^2) and the roots mean square error (RMSE). Also, the Pearson's correlation test was used to measure how well the two CHM's are related.

Tree height extraction

The tree height extraction involved two steps. Firstly the matching of the tree location information collected in the field with corresponding tree crown. Using the very high-resolution orthophoto generated from the UAV images the tree crowns within the plot were delineated by hand through photo interpretation. The tree location was inspected to ensure they fall within the peak of the corresponding tree crown. Using the Arc GIS the tree height (Z-value) of each tree were extracted from both UAV-CHM and LiDAR-CHM using add surface information function of 3D analyst tool.

3.4.4. AGB and carbon stock estimation

The allometric equation is a widely used method for estimating forest aboveground biomass and carbon stock in the tropical forest through non-destructive methods. These equations are developed by establishing a relationship between the various field measurable physical parameters of the trees such as the DBH, tree height, crown diameter, tree species and biomass through non-destructive method (Breu et al., 2012). Concerning the nature of the AHFR with diverse of tree species the generic allometric equation developed by Chave et al., (2014) to estimate AGB of the tree across forest types and use wood specific gravity, DBH and tree height as input parameters were adopted in this study(Equation 1-1). Adapting generic allometric equation have a potential to increase the precision of the AGB estimation and carbon stock as it takes into consideration a number of tropical forests-specific conditions include the diverse of tree species (Basuki et al., 2009). In this study, species-specific wood density was used for most of the tree species while the trees that the specific wood density was missing a recommended average wood density 0.57g/cm3 was applied (Schade & Ludwig, 2013).

For calculating the carbon stock the conversion factor (CF) was used to convert the AGB into carbon stock by multiply by the CF of 0.47(IPCC, 1996).Hence, calculating carbon stock the following equation was used:

Equation 3-2: Calculation of Carbon stock from AGB

$$C=AGB \times CF \quad \text{Equation 2}$$

Where

C: represent the Carbon stock (Mg C)
CF: is a fraction of above-ground biomass (0.47)
AGB: is Aboveground Biomass

3.4.5. Statistical analysis

The regression analysis is the most common method for studying the relationship between two or more variables. The forestry studies commonly use regression tests which provide the quantitative relationship and expressed by an equation, regression coefficients, and coefficient of determination (Kahyani et al., 2011). The coefficient of determination (R^2) and the root mean error square (RMSE) were used to represent the performance of the derived inputs forestry parameters of the allometric equation for estimation of AGB and carbon stock. The linear regression was used to assess the relationship between the field measured DBH and DBH extracted from TLS data, Field measured tree height and tree height extracted from TLS data for a lower canopy. Then assess the relationship between the tree height extracted from UAV CHM and tree height extracted from ALS CHM followed by assessing the relation between the total AGB estimated on plot base from TLS data and CHM from 3D image matching of UAV imagery versus the field measurements and height from ALS-CHM.
According to Sherali et al., (2003) compare the closeness of the two measurements of the forestry parameters the RMSE and percentage root mean square error (%RMSE) were calculated as follows:

Equation 3-3: Equation for RMSE and %RMSE calculation

$$RMSE = \sqrt{\sum_{i=1}^{n} (y_i - \hat{Y})^2 / n} \quad \text{.....Equation 3}$$

$$\%RMSE = RMSE * n * 100 / \sum Y_i \quad \text{.....Equation 4}$$

Source: (Sherali et al., 2003)
Where;

Y_i: Measured value of the Dependent variable
$\dot{i}$: Estimated the value of the dependent variable
n: Number of samples
RMSE: Root Mean Square Error of the relationship
%RMSE: Percentage Root Mean Square Error of the Relationship

Also, the F-test for two samples variance was carried out to determine which t-test to use to detect the difference between the means of the measured parameters and estimated AGB and carbon stock from two methods. The t-test is powerful to detecting differences between the two variables and observe if there is a significant difference between the means (Wang & Glenn, 2008).

4. RESULTS

4.1. DSM and Orthophoto Generation from UAV images

The DSM and ortho-mosaic image were generated using Agisoft Photoscan software through automatic 3D image matching method. Ground control points (GCPs') were used to assist spatial referencing of the 3D model generated from the UAV images. A total of 132.4 hectares were covered by the six flight blocks where the ortho-mosaic image with ground resolution ranges from 3.13 - 3.72 cm/pixel and DSMs' of 1m pixel resolution were generated. Some particular information on the UAV image processing conducted in Agisoft Photoscan is presented in Table 4-1 below. Also, a sample of generated DSM and ortho-mosaic image are illustrated in Figure 4-1 and Figure 4-2 below.

Table 4-1: Summary of UAV-image processing report using Agisoft Photoscan Professional

Flight block	Number of Used Images	Average Flying altitude (m)	Orthomosaic area (ha)	Point density (points/m²)	GCP's RMSE (pix)	Mean re-projection error(pixel)	Orthomosaic Ground resolution
1	234	105	17.7	180	0.42	1.06	3.72 cm/pix
2	215	95.2	17.9	202	0.41	0.861	3.52 cm/pix
3	140	90.1	14.3	254	0.44	1.21	3.13 cm/pix
4	638	95.6	35.9	50	0.44	1.03	3.53 cm/pix
5	557	94.3	36.1	217	0.43	0.973	3.4 cm/pix
6	191	96.7	10.5	210	0.40	0.576	3.45 cm/pix

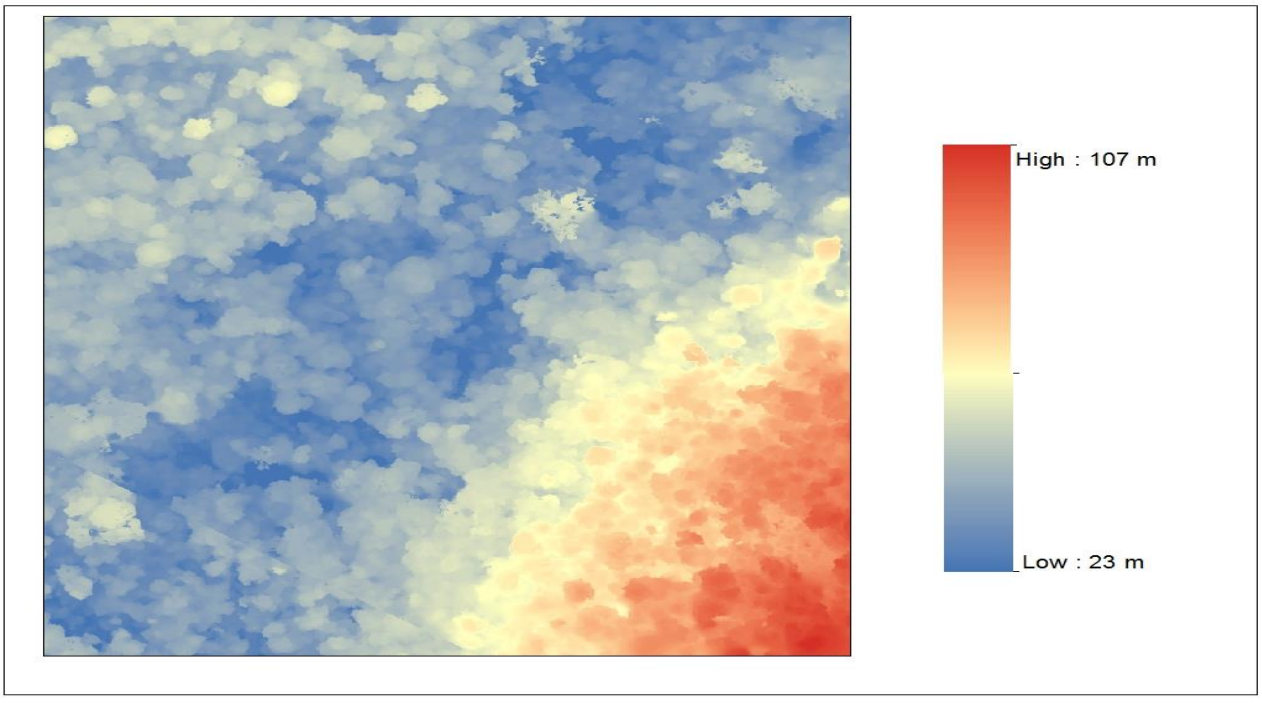

Figure 4-1: Small part of the DSM generated from the UAV images

Figure 4-2: Small part of the ortho-mosaic image generated from the UAV images

4.2. CHM Generation from Photogrammetric matching of UAV images

The CHM was generated by subtracting LiDAR DTM from the UAV DSM. The LiDAR-based DTM, which was built by Sadadi, (2016) was used in this study. The DTM pixel value was subtracted (Figure 4-3) from the corresponding UAV-DSM pixel value by using the Raster calculator in ArcGIS 10.4.1 software to produce the UAV-CHM which represent the absolute height of trees in the area.

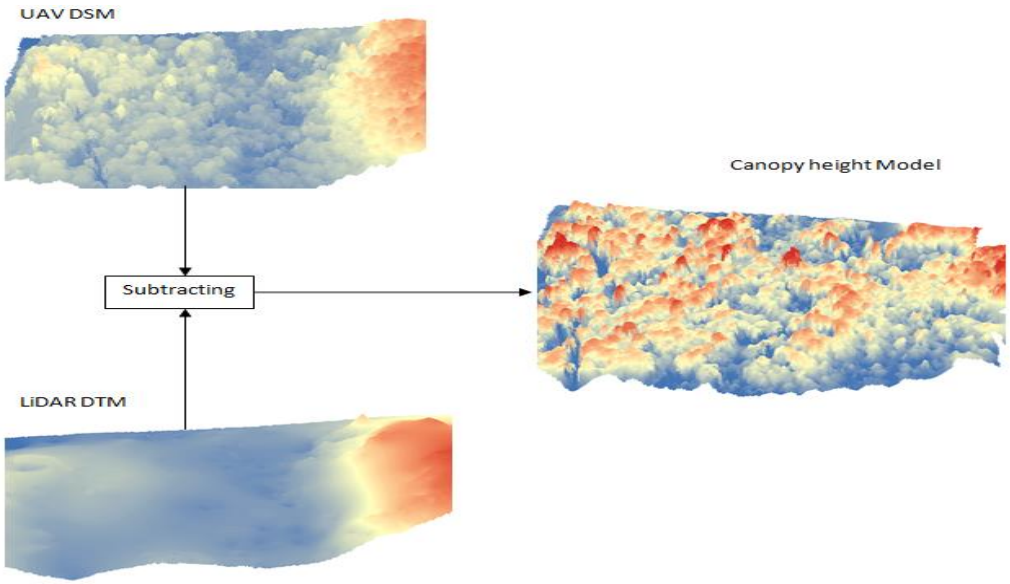

Figure 4-3: Generation of CHM from the UAV-DSM and LiDAR-DTM

4.3. Extraction and Assessment of tree height derived from UAV images

4.3.1. Extraction of Trees heights from UAV-CHM and ALS-CHM

The upper canopy trees were separated from lower canopy trees based on the thresholds that were set for separation as described in section 3.5.1. A total number of 524 upper canopy trees were extracted from the UAV and ALS canopy height models, out of 524 trees 6 of them were removed as outliers and reduced the number of trees to 518 trees which were used for comparison of the upper canopy tree height.

4.3.2. Descriptive statistics for upper canopy tree height

Descriptive statistics was conducted for both heights extracted from UAV-CHM and ALS-CHM for upper canopy trees. The mean height of 19.90 m and 18.64 m was recorded from UAV-CHM and ALS-CHM extracted tree height respectively and other descriptive statistics of the extracted trees are shown in Table 4-2. Also, the distributions of the data are illustrated in Appendix 3.

Table 4-2: Descriptive Statistics of UAV and ALS extracted tree height

	N	Range	Minimum	Maximum	Mean	Std. Deviation
ALS measured Height	518	31.71	8.06	39.77	18.64	4.69
UAV measured Height	518	28.84	8.96	37.80	19.90	4.82

4.3.3. Relationship between the tree heights extracted from UAV–CHM and ALS-CHM

A total of 518 trees were used to assess the tree heights derived from UAV-CHM and ALS-CHM for the upper canopy layer. The scatter plot illustrate the relationship between the UAV-CHM and ALS-CHM extracted heights (Figure 4-4) showed a strong correlation of 0.90 and coefficient of determination (R^2) of 0.81. The root mean square error (RMSE) was 2.1m which are equivalent to 11% of the total estimated tree height from UAV-CHM (Table 4-3).

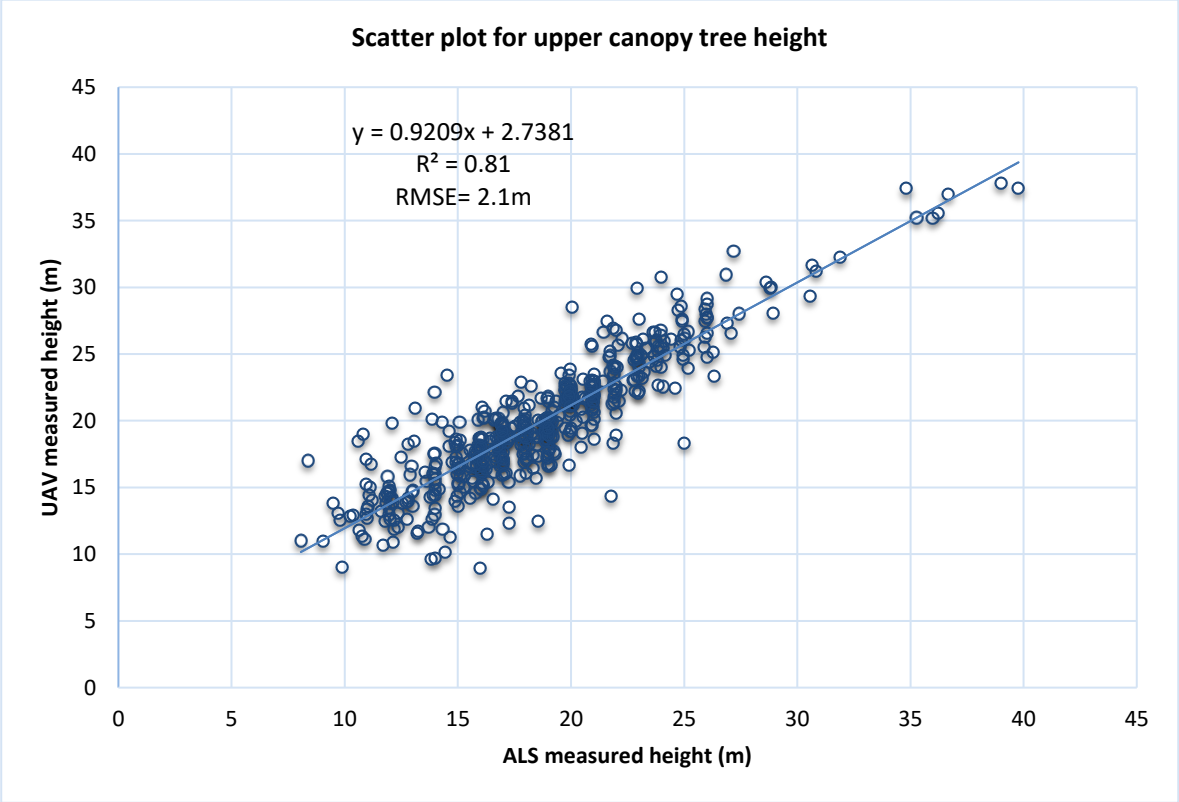

Figure 4-4: The scatter plot of ALS-CHM and UAV-CHM extracted upper canopy tree height

Table 4-3: Regression Statistics, probability of ALS-CHM and UAV-CHM extracted upper canopy tree height

Pearson Correlation	R Square	Adjusted R Square	RMSE (m)	RMSE (%)
0.90	0.81	0.80	2.10	11

	Coefficients	Standard Error	t -Stat	P-value
Intercept	1.2404	0.388	3.199	0.001465
ALS height	0.8742	0.019	46.159	2.50E-185

4.3.4. F-test two sample for variance

The F-test was conducted to find out if the two samples (ALS-CHM and UAV-CHM extracted upper canopy tree heights) have an equal variance or unequal variance, in order to determine which t-test to use to detect the difference between the two methods. The results of the F-test shows equal variance between the two samples see Table 4-4 where the F-statistic < F-critical (P> 0.05). Therefore a t-test assuming equal variance was conducted.

Table 4-4: F-test of two samples for variance

	UAV Height	ALS Height
Mean	19.90	18.64
Variance	23.20	22.02
Observations	518.00	518.00
Df	517.00	517.00
F-Stat	1.05	
P(F<=f) one-tail	0.28	
F Critical one-tail	1.16	

Decision: F-statistic < F-critical (P> 0.05): Equal variance

4.3.5. T-test assuming equal variance

To find out if there is a significance difference between the tree heights extracted from UAV-CHM and ALS-CHM a t-test assuming equal variance was conducted. The results (Table 4-5*)* shows that there is significance difference between the two methods where t-statistic > t-critical (p<0.05).

Table 4-5: The t-test assuming unequal variance for ALS and UAV extracted upper canopy tree height

	UAV Height	ALS Height
Mean	19.90	18.64
Variance	23.20	22.02
Observations	518.00	518.00
Df	1034.00	
t Stat	4.28	
P(T<=t) two-tail	0.00002	
t Critical two-tail	1.96	

Decision: T-statistic > T-critical (p<0.05): The null hypothesis was rejected, so there is a significance difference between the two means.

4.4. TLS data processing

4.4.1. Registered Scans

The multiple scan positions for each plot were registered to the corresponding center scan position which presents the project coordinate system. The multiple station adjustment was obtained with high accuracy where the standard deviation error of the registered multiple scans for all 30 plots range between 0.019m and 0.038m with an average of 0.024m (Table 4-6).

Table 4-6: Summary of standard deviation error of Registration of Scans

Plot No.	1	2	3	4	5	6	7	8	9	10
Standard deviation (m)	0.019	0.023	0.024	0.022	0.028	0.025	0.038	0.023	0.023	0.020
Plot No.	11	12	13	14	15	16	17	18	19	20
Standard deviation (m)	0.029	0.021	0.025	0.022	0.021	0.023	0.026	0.0201	0.0248	0.0217
Plot No.	21	22	23	24	25	26	27	28	29	30
Standard deviation (m)	0.024	0.028	0.024	0.026	0.021	0.024	0.022	0.019	0.029	0.033

4.4.2. Individual tree extraction

The extracted plot was displayed on liner true colour to enhance visualization of the tree tags for individual tree identification. The individual tree extraction involved detection and identification of individual trees using the tree tag number followed by manual separation of individual tree and stored as polydata. The extracted individual trees were further processed by extracting the tree parameters such as DBH and height using the RiSCAN PRO software. The extracted forest parameters were recorded in Microsoft Excel sheet for further analysis. Out of the 924 tagged trees in the field, 854 could be extracted from the TLS point clouds see Table 4-7 below.

Table 4-7: Summary of trees extracted from TLS point clouds

No of plots	Field recorded	TLS derived	Extracted (%)	Missing trees (%)
30	924	854	92.4	7.6

4.5. The lower canopy tree height

A total number of 330 trees separated to lower canopy based on the thresholds set up using the TLS measured height (12 m for multi-layered plots and 8 m for the less complex or single layer plots) that was a set up to separate the lower canopy from the upper canopy. Out of the 330 lower canopy trees, a total of 13 trees were removed as outliers because they were not well captured by the TLS due to the intermingling of the tree canopy.

4.5.1. Descriptive statistics for lower canopy tree height

Descriptive statistics was conducted for 317 trees for both heights measured in the field and derived from the TLS data for lower canopy trees. The mean tree height of 9.72 m and 9.55 m was recorded from field and TLS respectively and other descriptive statistics of the sampled trees are shown in Table 4-8. Also, the lower canopy tree height data appear to follow a normal distribution curve (Appendix 2). The maximum height measured by the TLS was 12 m for lower canopy because the TLS height was used to set the threshold where 12m was a threshold for the multi-layered plot to separate the lower canopy from the upper canopy. The highest value for the field value is 16 m see Table 4-8. This can be attributed to errors of measuring

height with a handheld instrument device in the field. The small experiment conducted in ITC prior to field work shows that TLS measurement sets are very accurate and trees height measured with a handheld instrument device are unreliable, particularly in a situation with a complex forest structure.

Table 4-8: Descriptive Statistics of field and TLS measured height for Lower canopy

		N	Range	Minimum	Maximum	Mean	Std. Deviation
TLS Height	Measured	317	7.50	5.00	12.00	9.55	1.82
Field Height	Measured	317	12.00	4.00	16.00	9.72	2.59

4.5.2. Relationship between tree height measured in the Field and derived from TLS

A total of 317 trees were used to assess the relationship between the TLS derived height and field-measured tree height in the lower canopy. The linear regression of TLS derived height and field measured height (Figure 4-5) shows a correlation of 0.83 and coefficient of determination (R^2) of 0.69.The root mean square error (RMSE) was 1.4 m which are equivalent to 15% of the total height measured in the field see Table 4-9. It also clearly showed by the experiment that the deviation from the regression line increase with increasing height, which based on the accuracy assessment of the TLS and tree measurements with a handheld device.

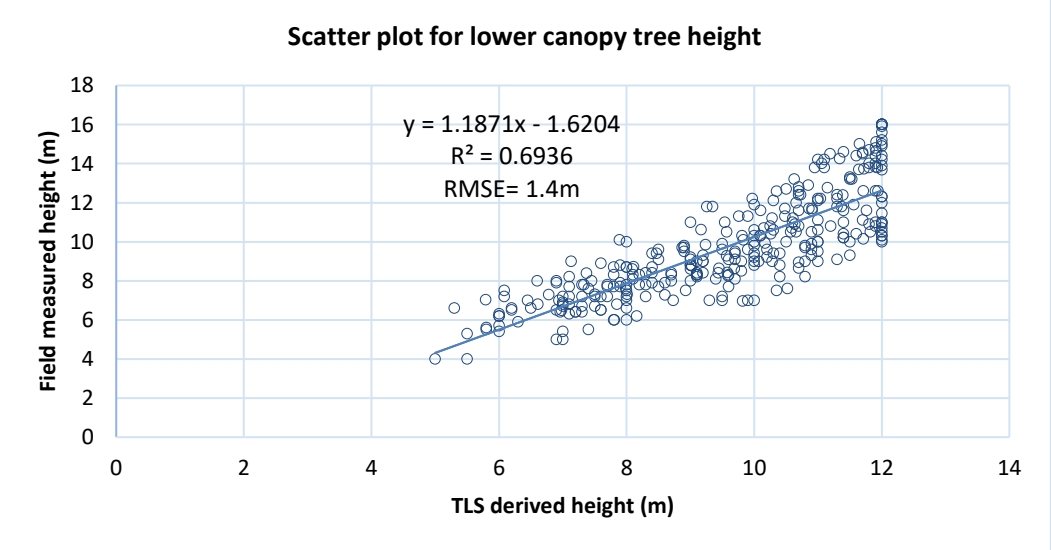

Figure 4-5: The scatter plot of TLS derived height and field measured height

Table 4-9: Regression Statistics, probability of Field and TLS extracted lower canopy tree heights

Pearson Correlation	R Square	Adjusted R Square	RMSE (m)	RMSE (%)
0.83	0.69	0.69	1.4	15

	Coefficients	*Standard Error*	*t Stat*	*P-value*
Intercept	-1.62	0.432	-3.7497	0.00021
X Variable 1	1.187	0.0445	26.7051	$6.53x10^{-83}$

4.5.3. F-test two sample for variance

F-test for two samples was used to determine which t-test to use to detect if there is a significance different between the two samples. The results of the F-test shows unequal variance between the two samples (Table 4-10) where the F-statistic > F-critical (P< 0.05).

Table 4-10: F-test of two samples for variance

	Field Height	TLS Height
Mean	9.72	9.55
Variance	6.71	3.30
Observations	317.00	317.00
Df	316.00	316.00
F-statistic	2.03	
P(F<=f) one-tail	$2.3x10^{-10}$	
F Critical one-tail	1.20	

Decision: F-statistic is > F-critical (p<0.05), unequal variance

4.5.4. T-test assuming unequal variance

To find out if there is significance difference between the tree height measured direct in the Field and derived tree height from TLS a t-test assuming unequal variance was conducted. The results (Table 4-11) shows that there is no significance difference between the two tree measured in the field and derived from TLS where t-statistic < t-critical (p>0.05).

Table 4-11: The t-test assuming unequal variance for Field and TLS extracted lower canopy tree height

	Field Height	TLS Height
Mean	9.72	9.55
Variance	6.71	3.30
Observations	317.00	317.00
Df	566.00	
T-Stat	0.94	
P(T<=t) two-tail	0.35	
T Critical two-tail	1.96	

Decision: t-statistic is < t-critical (p>0.05), There is no significance difference

4.6. The tree DBH measured in the Field and derived from TLS

A total of 70 trees were removed from the data collected in the field because they were not captured by the TLS or missed during individual trees extraction and thus the number of trees used for analysis was reduced to 854 trees.

4.6.1. Descriptive analysis of Field and TLS measured DBH

Descriptive statistics was conducted for both DBH measured in the field and DBH derived from the TLS data. The mean DBH of 20.87cm and 20.59 cm was recorded from the field and TLS measured DBH respectively. Other descriptive statistics of the sampled trees are shown in Table 4-12. Also, the distribution of the data shows the positive skewness (Appendix 1).

Table 4-12: Descriptive Statistics of field and TLS measured DBH

	Number of trees	Minimum DBH	Maximum DBH	Mean	Std. Deviation
Field DBH (cm)	854	10.00	84.00	20.87	11.52
TLS DBH (cm)	854	9.0	83.6	20.59	11.48

4.6.2. Relationship between DBH measured in the Field and derived from TLS

A total of 854 trees that were both measured in the field and derived from the TLS points cloud were used to assess the relationship between the DBH measured in the field and the DBH derived from the TLS points cloud. The relationship was presented by the correlation coefficient (r), the coefficient of determination (R^2) and root mean square error (RMSE). The scatter plot of field measured DBH and TLS derived DBH (Figure 4-6) shows a strong correlation(r) of 0.99 and coefficient of determination (R^2) of 0.986. The root mean square error (RMSE) was 1.4 cm which is equivalent to 7% of the total DBH derived from TLS point clouds see Table 4-13.

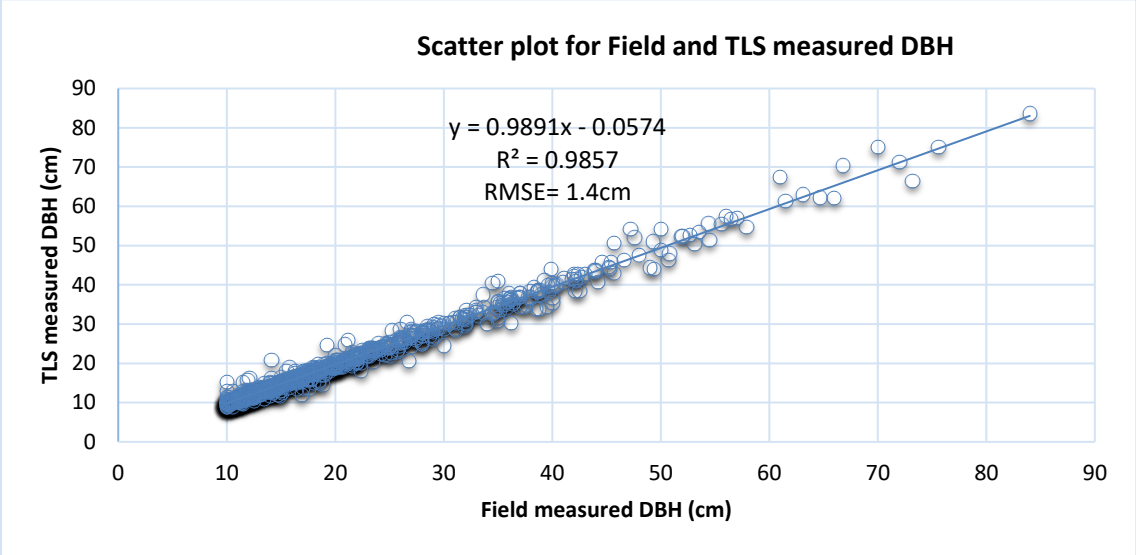

Figure 4-6: The scatter plot of field measured DBH and TLS derived DBH for upper and lower canopy

Table 4-13: Regression Statistics, probability of the Field and TLS measured DBH

Pearson Correlation	R Square	Adjusted R Square	RMSE (cm)	RMSE (%)
0.99	0.986	0.986	1.4	7
	Coefficients	*Standard Error*	*t Stat*	*P-value*
Intercept	-0.057	0.098	-0.585	0.558986
X Variable 1	0.989	0.0041	240.043	0

4.6.3. F-test two sample for variance

To determine which t-test to use, F-test for two samples was conducted. The results showed equal variance between the field and TLS measured DBH (Table 4-14) where the F-statistic < F-critical (P> 0.05).

Table 4-14: F-test of two samples for variance

	Field DBH (cm)	TLS DBH(cm)
Mean	20.87	20.59
Variance	132.74	131.75
Observations	854.00	854.00
Df	839.00	839.00
F-statistic	1.01	
P(F<=f) one-tail	0.46	
F Critical one-tail	1.12	

Decision: F-statistic is < F-critical (p>0.05), equal variance

4.6.4. T-test assuming unequal variance

To find out if there is significance difference between the tree DBH measured direct in the field and derived tree DBH from TLS point clouds a t-test assuming equal variance was conducted. The results (Table 4-15) show that there is no significance difference between the two tree measured in the field and derived from TLS where t-statistic < t-critical ($p>0.05$).

Table 4-15: The t-test assuming equal variance for Field and TLS measured DBH

	Field DBH(cm)	TLS DBH(cm)
Mean	20.87	20.59
Variance	132.74	131.75
Observations	854.0	854.0
Df	1678.0	
t Stat	0.51	
P(T<=t) two-tail	0.61	
t Critical two-tail	1.96	

Decision: t-statistic is < t-critical ($p>0.05$), There is no significance difference

4.7. Lower canopy AGB and carbon stock

The AGB for lower canopy layer was calculated using the allometric equation (Equation 1-1) using parameters derived from TLS (DBH, height) and field measured parameters (DBH and height) and species-specific wood density (Appendix 8) as well as average wood density 0.57g/cm^3 for the trees that their specific species wood density was missing. The same allometric equation was applied to calculate the lower canopy AGB for Reference using field measured DBH and TLS derived tree height.

4.7.1. Relationship between the estimated Field and Reference AGB for lower canopy

The regression analysis was carried out to establish the relationship between the estimated Field AGB and Reference AGB (Field DBH and TLS derived height for lower canopy) for lower canopy layer. Also, the estimated Field AGB and Reference was compared and presented (Figure 4-9) by the bar chart for good visualization of the differences. The scatter plot illustrate the relationship between estimated Field AGB, TLS AGB against Reference for lower canopy (Figure 4-6) shows a very strong correlation of 0.98 and 0.99, the coefficient of determination (R^2) of 0.97 and 0.99 respectively. The root mean square error (RMSE) was 45.01Kg and 28.6Kg which is equivalent to 7% and 4.7% of the total observed lower canopy AGB for plots respectively (Table 4-16).

Table 4-16: Regression Statistics, probability for lower canopy estimated AGB

	Pearson Correlation	R Square	RMSE (Kg)	RMSE (%)
TLS against Reference	0.99	0.99	28.6	4.7
Field against Reference	0.98	0.974	45.01	7
TLS against Field	0.97	0.968	50.7	8

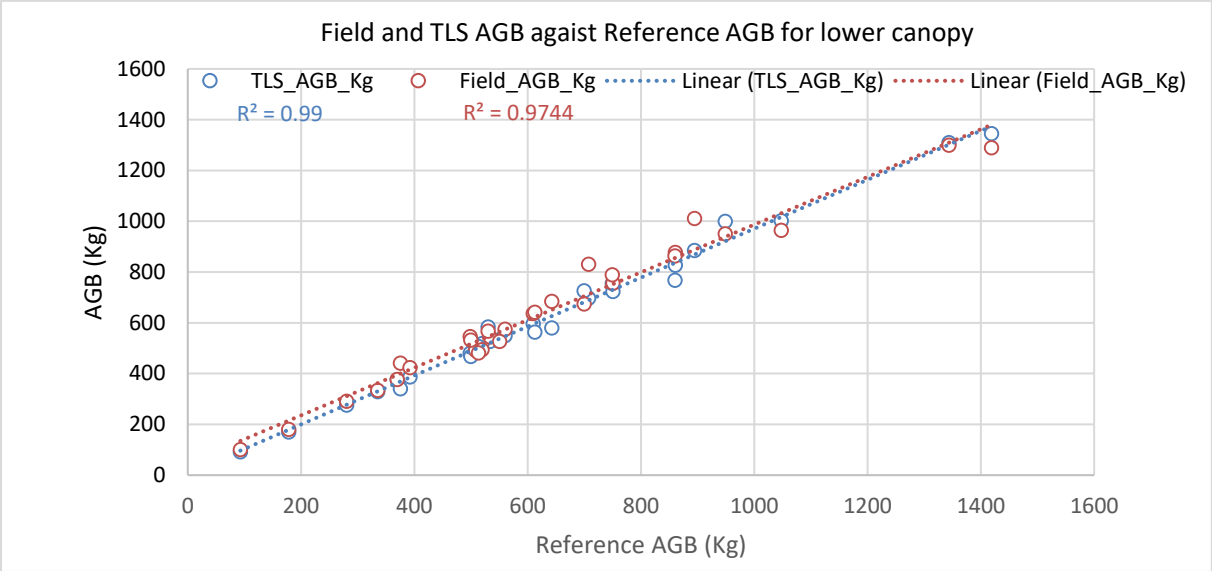

Figure 4-7: The scatter plot showed the relationship of Field and TLS against Reference AGB for lower canopy

Table 4-17: Regression Statistics, probability for lower canopy estimated AGB

Pearson Correlation	R Square	Adjusted R Square	RMSE (Kg)	RMSE (%)
0.98	0.97	0.966	45.01	7
	Coefficients	Standard Error	t Stat	P-value
Intercept	45.75936	22.67133	2.01838	0.053223
TLS AGB (Kg)	0.966354	0.033485	28.85969	$2.25x10^{-22}$

4.8. Upper canopy AGB and carbon stock

The AGB for upper canopy layer was calculated using the allometric equation (Equation 1-1) and the input parameters were the tree DBH derived from the TLS cloud points, height extracted from UAV-CHM (TLS&UAV) and species-specific wood density as well as average wood density 0.57g/cm3 for the trees that their species-specific wood density was missing. The same allometric equation was applied to calculate the Reference AGB using field measured DBH and tree height extracted from ALS-CHM (Field & ALS).

4.8.1. Comparison between TLS & UAV and Reference estimated AGB for upper canopy

The regression analysis was conducted to establish the relationship between developed method (TLS DBH & UAV tree height) and reference (Field DBH & ALS tree height) estimated AGB for upper canopy layer. Also, the estimated AGB for developed method and reference were compared and presented (Figure 4-9) by the bar chart for good visualization of the difference. The scatter plot showed the relationship between estimated developed method and reference AGB for upper canopy (Figure 4-8) shows a very strong correlation of 0.99 and coefficient of determination (R^2) of 0.98. The root mean square error (RMSE) was 524Kg which is equivalent to 7% of upper canopy AGB for 30 plots (Table 4-18).

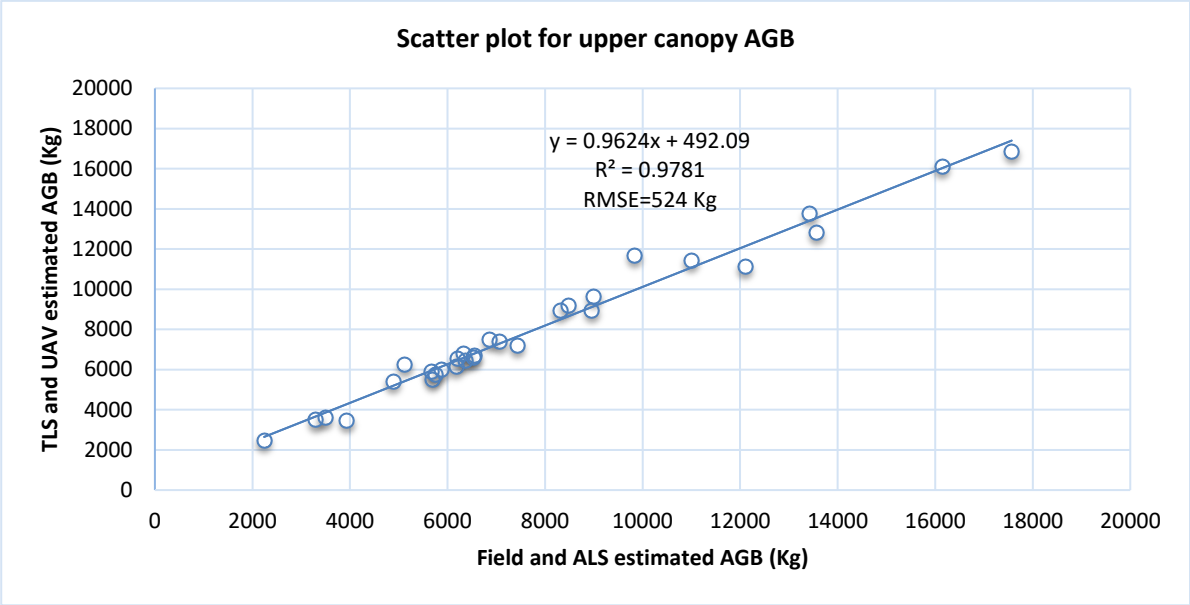

Figure 4-8: Scatter plot shows the relationship of estimated AGB of Field & ALS and TLS&UAV for upper canopy

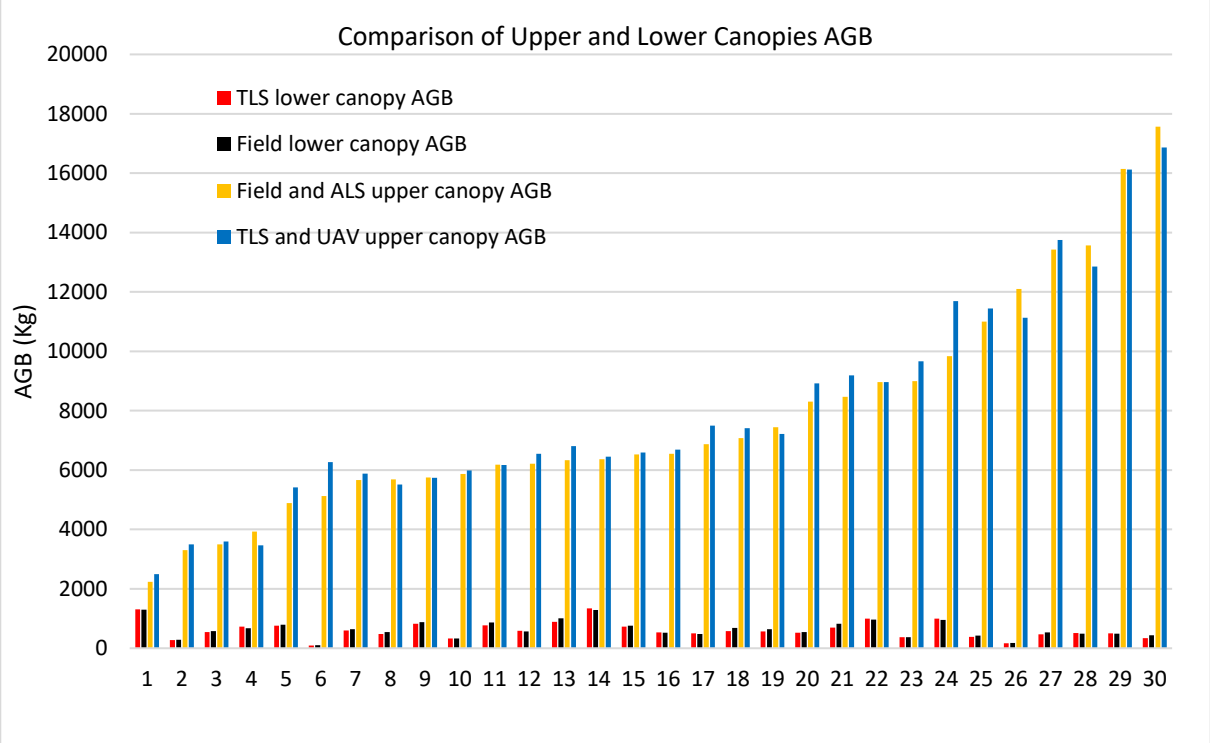

Figure 4-9: Comparison of estimated AGB of developed and referenced methods for upper and lower canopies

Table 4-18: Regression Statistics, probability for upper canopy estimated AGB

Pearson Correlation	R Square	Adjusted R Square	RMSE (Kg)	RMSE (%)
0.99	0.98	0.98	524.5	7
	Coefficients	Standard Error	t-Stat	P-value
Intercept	492.0906	234.1821	2.101316	0.044739
X Variable 1	0.962416	0.027217	35.3606	8.83×10^{-25}

4.9. The total AGB and carbon stock estimated on plot base

Developed method based on the modern remote sensing technology (UAV and TLS) was compared with three methods to test the effects of forest parameters on AGB/carbon at plot level

1. TLS and ALS estimated AGB.
2. Field and ALS estimated AGB.
3. Reference (Field DBH + TLS lower canopy height+ ALS upper canopy height) estimated AGB.

The overall AGB was calculated by combining the upper and lower canopy AGB for each plot. The summation of the TLS & UAV estimated AGB for the upper canopy and the lower canopy was calculated, likewise, the summation of the estimated AGB for the comparable methods was calculated. A total carbon stock per plot was calculated (Equation 3-2) by multiply a total AGB per plot with the conversion factor of 0.47 (IPCC, 1996). The summary of the overall AGB and carbon stock are shown in Table 4-24.

4.9.1. Descriptive analysis of Overall AGB and carbon stock

Using SPSS the descriptive statistics (Table 4-19) was carried out for the overall AGB and carbon stock

Table 4-19: Descriptive Statistics of total AGB and Carbon stock for the 30 plots

	N	Range	Minimum	Maximum	Mean	Std. Deviation
Total UAV & TLS AGB (Kg)	30	13432.6	3769.5	17202.11	8608.75	3532.31
Total TLS & ALS AGB (Kg)	30	14358.86	3549.83	17908.69	8409.67	3626.85
Total Field & ALS AGB (Kg)	30	14469	3539.89	18008.89	8434.78	3631.46
Total Field, ALS & TLS AGB (Kg)	30	14361.17	3582.34	17943.52	8425.44	3627.73
Total UAV&TLS Carbon stock (Mg)	30	6.31	1.77	8.08	4.05	1.66
Total TLS&ALS Carbon stock (Mg)	30	6.75	1.67	8.42	3.95	1.70
Total Field & ALS Carbon stock (Mg)	30	6.80	1.66	8.46	3.97	1.71
Total Field, ALS&TLS Carbon stock (Mg)	30	6.75	1.68	8.43	3.96	1.71

4.9.2. Comparison of the overall AGB for the 30 plots

The overall estimated AGB for the developed method, reference method and the two optional methods for assessing the individual parameters were compared and presented by the bar chart (Figure 4-10) for good visualization of the difference. The comparison between the developed method and:-

1. Reference (Field DBH + TLS lower canopy height+ ALS upper canopy height) estimated AGB indicate the performance of the developed method.
2. TLS and ALS estimated AGB shows the effect of tree height extracted from UAV-CHM on AGB at the plot level.
3. Field and ALS estimated AGB shows the uncertainty can be obtained when field measured height for lower canopy AGB used as a reference.

Table 4-20: Regression Statistics, probability for the overall estimated AGB using various methods

	Pearson Correlation	R Square	RMSE (Kg)	RMSE (%)
UAV &TLS Vs Reference	0.99	0.976	536.25	6.23
UAV &TLS Vs Field &ALS	0.99	0.988	530.14	6.16
TLS & UAV Vs TLS &ALS	0.99	0.988	525.32	6.10
TLS & ALS Vs Reference	0.99	0.99	30	0.004

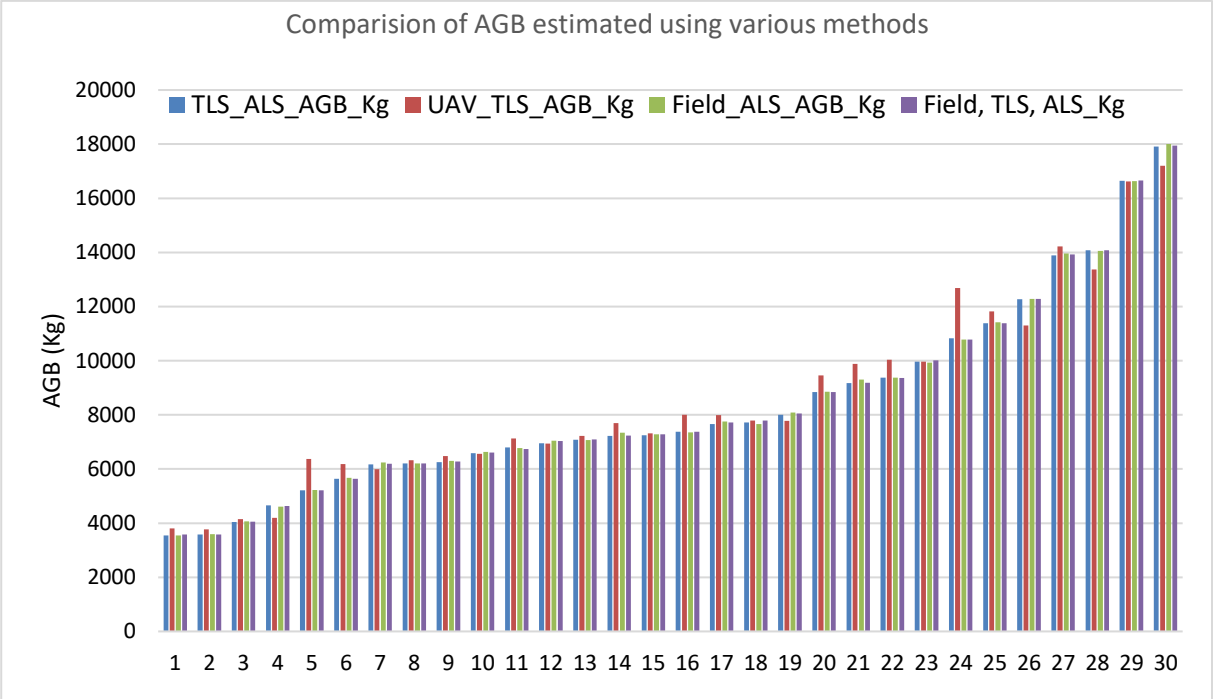

Figure 4-10: The comparison of the overall estimated Field & ALS and TLS&UAV AGB

4.9.3. Relationship between the overall AGB estimated TLS&UAV and Reference AGB

The regression analysis was conducted to establish the relationship between the overall estimated TLS & UAV AGB versus reference AGB at plot level (Figure 4-11). The result shows a strong correlation of 0.99 and coefficient of determination (R^2) of 0.988. The root mean square error (RMSE) was 536.25 Kg which is equivalent to 6.23% of the total AGB per plot for 30 plots (Table 4-21).

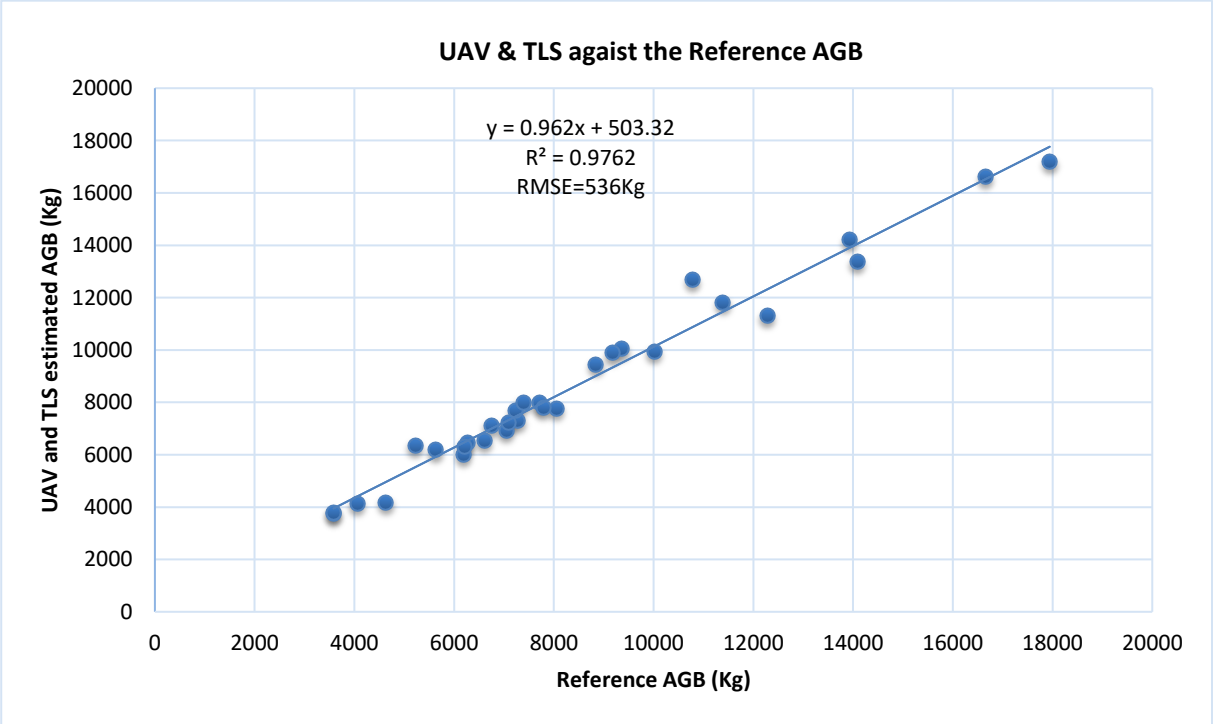

Figure 4-11: Scatter plot shows the relationship of the overall AGB of TLS&UAV and Reference on plot base

Table 4-21: Regression Statistics, probability for the overall estimated Field & ALS and TLS&UAV AGB

Pearson Correlation	R Square	Adjusted R Square	RMSE (Kg)	RMSE (%)
0.99	0.98	0.98	536.25	6.23

	Coefficients	Standard Error	T- Stat	P-value
Intercept	503.32	259.96	1.94	0.063001
Reference AGB	0.96	0.03	33.86	$2.9x10^{-24}$

4.9.4. F-test two sample for variance

The F-test was conducted to find out if the two samples have an equal variance or unequal variance. Hence to determine which t-test to use to detect the difference between the two methods. The results of the F-test shows that there is equal variance between the two samples see Table 4-22 where the F-statistic < F-critical (P> 0.05).

Table 4-22: F-test of two samples for variance

	Reference AGB (Kg)	UAV and TLS AGB (Kg)
Mean	8425.44	8608.75
Variance	13160455.07	12477222.04
Observations	30.00	30.00
Df	29.00	29.00
F-statistic	1.05	
P(F<=f) one-tail	0.44	
F Critical one-tail	1.86	

Decision: The F-statistic < F-critical (P> 0.05) Equal variance

4.9.5. T-test assuming equal variance

To find out if there is significance different between the AGB estimated using TLS & UAV data set and the reference data set, a t-test assuming equal variance was conducted. The results (Table 4-23) show that there is no significance difference between the two methods where t-statistic < t-critical (p>0.05).

Table 4-23: T-test for overall Field & ALS and UAV&TLS AGB

	Reference AGB (Kg)	UAV and TLS AGB (Kg)
Mean	8425.44	8608.75
Variance	13160455.07	12477222.04
Observations	30.00	30.00
Df	58.00	
t Stat	-0.20	
P(T<=t) two-tail	0.84	
t Critical two-tail	2.00	

Decision: The t-statistic < t-critical (P> 0.05) no significance difference

Table 4-24: Summary of the total AGB and Carbon stock for the 30 plots

Plot	Total Reference AGB (Metric Ton)	Total UAV&TLS AGB(Metric Ton)	Total Reference Carbon (Mg)	Total UAV&TLS Carbon (Mg)
1	5.22	6.37	2.45	2.99
2	7.28	7.32	3.42	3.44
3	7.72	7.99	3.63	3.76
4	9.37	10.04	4.40	4.72
5	9.18	9.89	4.31	4.65
6	8.84	9.45	4.16	4.44
7	17.94	17.20	8.43	8.08
8	6.27	6.47	2.95	3.04
9	7.23	7.69	3.40	3.62
10	5.63	6.18	2.65	2.90
11	6.61	6.56	3.11	3.09
12	8.05	7.78	3.78	3.66
13	6.19	6.00	2.91	2.82
14	10.01	9.96	4.70	4.68
15	12.28	11.30	5.77	5.31
16	4.63	4.19	2.18	1.97
17	16.66	16.62	7.83	7.81
18	14.08	13.37	6.62	6.28
19	6.74	7.13	3.17	3.35
20	7.38	8.00	3.47	3.76
21	11.39	11.83	5.35	5.56
22	13.92	14.22	6.54	6.68
23	10.78	12.69	5.07	5.96
24	7.04	6.94	3.31	3.26
25	7.09	7.23	3.33	3.40
26	6.21	6.32	2.92	2.97
27	4.05	4.15	1.91	1.95
28	3.58	3.77	1.68	1.77
29	3.58	3.81	1.68	1.79
30	7.79	7.79	3.66	3.66
Total	**252.76**	**258.26**	**118.80**	**121.38**
Average AGB and carbon stock per plot	**8.43**	**8.61**	**3.96**	**4.05**
Average AGB and carbon stock per hectares	**168.51**	**172.18**	**79.20**	**80.92**

4.9.6. Relationship between the overall AGB estimated TLS&UAV and Field & ALS AGB

The regression analysis was conducted to establish the relationship between the overall estimated TLS & UAV AGB versus Field & ALS AGB at plot level (Figure 4-12). The result shows a strong correlation of 0.99 and coefficient of determination (R^2) of 0.977. The root mean square error (RMSE) was 530.14Kg which is equivalent to 6.16% of the total AGB per plot for 30 plots see

Table 4-25. The results indicate the effect of the field measured lower canopy tree height using the handheld instrument on AGB at plot level when used as reference height.

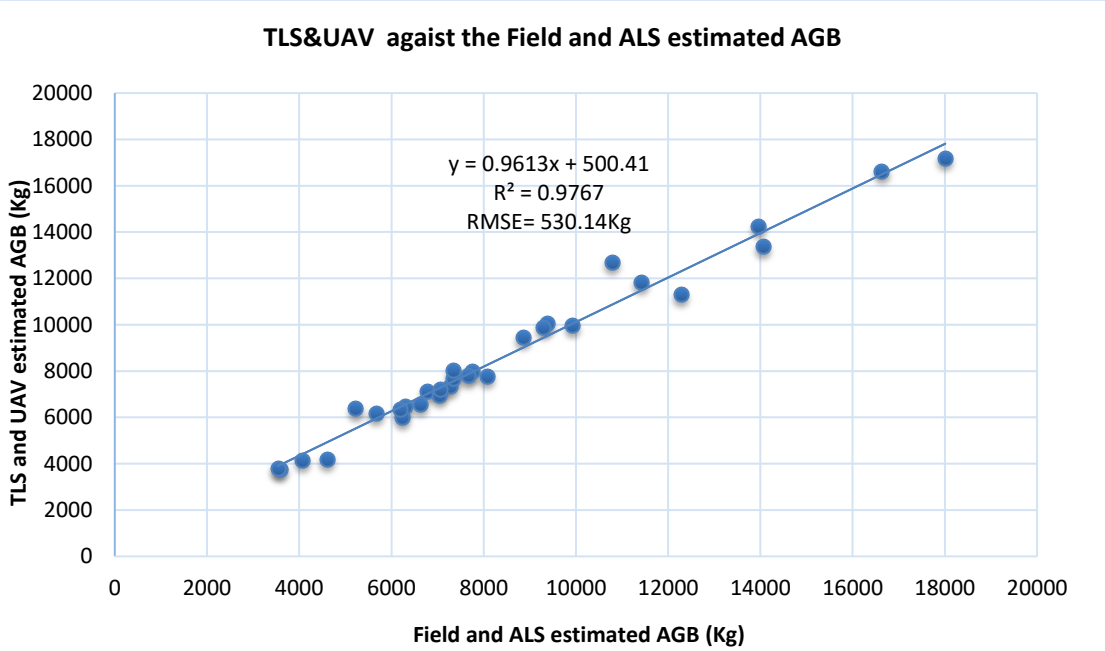

Figure 4-12: Scatter plot showed the relationship of the overall AGB of TLS&UAV and Field & ALS on plot base

Table 4-25: Regression Statistics, probability for the overall estimated TLS&UAV and Field & ALS AGB

Pearson Correlation	R Square	Adjusted R Square	RMSE (Kg)	RMSE (%)
0.99	0.98	0.98	530.14	6.16
	Coefficients	Standard Error	t Stat	P-value
Intercept	500.4094	257.0116	1.947031	0.062
Field &ALS AGB	0.961298	0.02806	34.25859	2.1×10^{-24}

4.9.7. Relationship between the overall AGB estimated TLS&UAV and TLS & ALS AGB

The regression analysis was conducted to establish the relationship between the overall estimated TLS & UAV AGB versus TLS & ALS AGB at plot level (Figure 4-13). The result shows a strong correlation of 0.99 and coefficient of determination (R^2) of 0.977. The root mean square error (RMSE) was 525.32 Kg which is equivalent to 6.10% of the total AGB per plot for 30 plots (Table 4-26).This result shows the effect of the upper canopy height extracted from the UAV-CHM to AGB at the plot level.

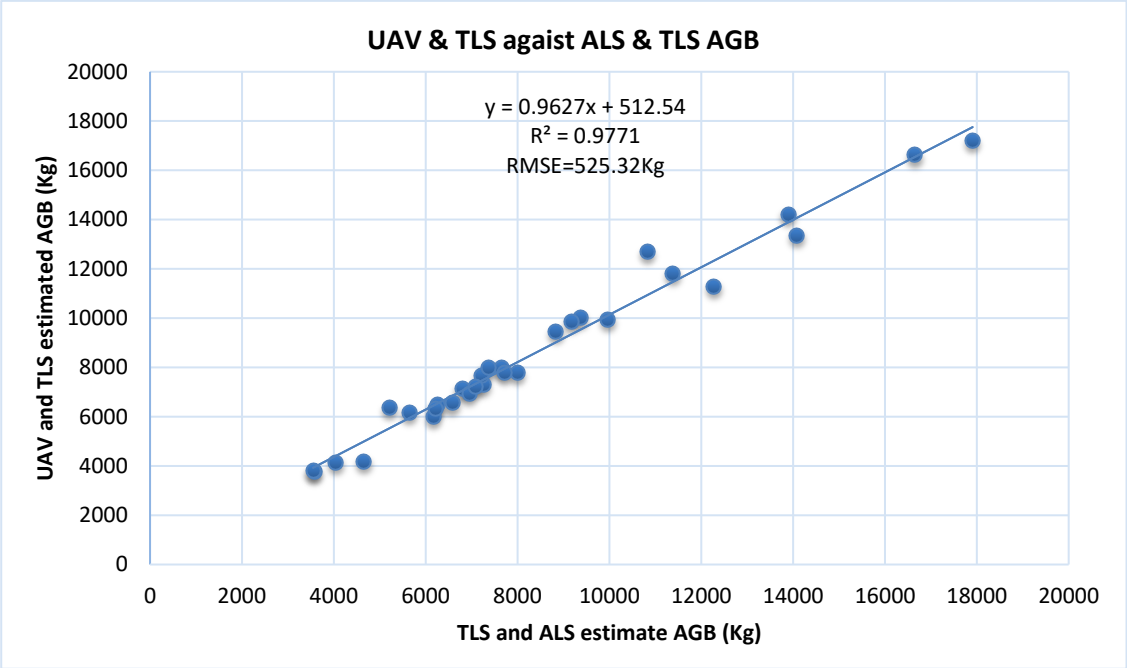

Figure 4-13: Scatter plot shows the relationship of the overall AGB of TLS&UAV and TLS & ALS on plot base

Table 4-26: Regression Statistics, probability for the overall estimated TLS&UAV and TLS & ALS AGB

Pearson Correlation	R Square	Adjusted R Square	RMSE (Kg)	RMSE (%)
0.988	0.977	0.976	525.32	6.10
	Coefficients	Standard Error	t Stat	P-value
Intercept	512.54	254.31	2.02	0.053546
TLS &ALS AGB	0.96	0.03	34.58	$1.63x10^{-24}$

5. DISCUSSIONS

5.1. Descriptive analysis of measured forestry parameters

The distribution of both TLS and field-measured tree DBH and height were analyzed. The results show that the DBH measured from the field using DBH tape and DBH derived from the TLS point cloud were not normally distributed (Appendix 1) and were positive skewed see (Figure 5-1). The distribution of field and TLS DBH were both positive skewed because only trees with DBH greater or equal to 10 cm were measured. While the trees with DBH less than 10 cm were excluded from this study with the assumption that, they often contribute very little on the total forest AGB (Brown, 2002).
Also, the TLS height was not normally distributed because the TLS height was used to set up the threshold to separate lower canopy from the upper canopy. Therefore, the trees with a height greater than 12m were considered as upper canopy trees. The field height appeared to follow the normal distribution curve (Appendix 2). On the other hand, both tree height extracted from the UAV-CHM and ALS-CHM appeared to follow the normal distribution curve (Appendix 3).

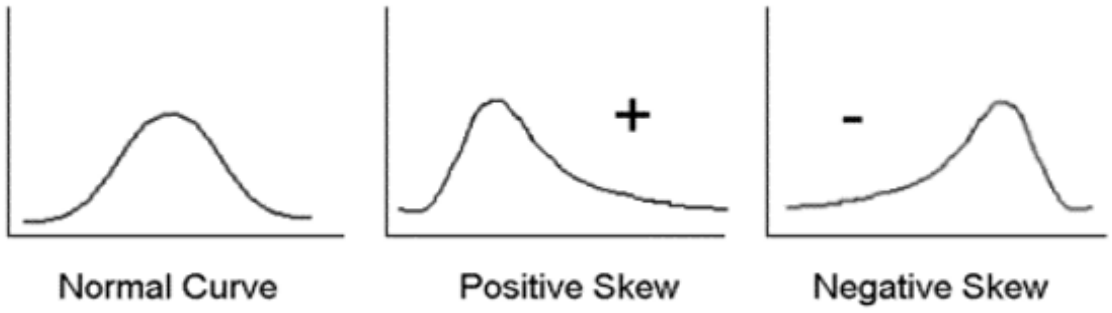

(Source: ***http://allpsych.com/researchmethods/distributions***)

Figure 5-1: Normal and Skewed curves

5.2. Comparison between UAV-CHM and ALS-CHM extracted tree height for Upper canopy

The UAV images were processed through automatic 3D image matching approach using the Agisoft Photoscan software to produce orthophoto (true colour high-resolution image) and Digital Surface Model (UAV-DSM) as described in this study on section 3.5.3. Some of the previous studies used this software to process UAV images to generate high-resolution DSM and ortho-mosaic (Aicardi et al., 2016, Leon et al., 2015, Gomez et al., 2015). The root mean square error (RMSE) of GCPs' estimated coordinates was less than 2 cm for the generated 3D model that was used to generate accurate DSM and orthophoto. This is a reasonably accurate result achieved by the images acquired by UAV with strong overlap condition and GCPs' measured with high accuracy Differential GPS for geo-referencing the 3D model.

The UAV-CHM was generated by subtracting LiDAR-DTM from the UAV-DSM. To assess the accuracy of generated UAV-CHM the tree height was extracted from both two data set for comparison.

A total of six trees were eliminated as an outlier because the extracted heights were extremely underestimated by UAV-CHM. These trees were assessed through visual interpretation from the orthophoto and some of the trees measured by ALS when they were alive, observed broken and fallen (Figure 5-2). Therefore, the fall of the large trees open up the canopy and expose the lower canopy trees and viewed by the UAV as upper canopy which causes a high discrepancy of the tree heights extracted from the two canopy height models. This situation was reported by Nurul-Shida et al., (2014)study, which clarify the fall of the big trees

in AHFR especially during the monsoon season with heavy rainfall and its damaging effects on the trees standing nearby which results to a gap creations at large scale.

Figure 5-2: Example of observed tree broken/fallen and its damaging effects on the adjacent trees

Also, the mean tree height difference between the trees extracted from the UAV-CHM and ALS-CHM for this plot showed that the UAV-CHM underestimated the tree height by approximately 1m (Appendix 5), which may be the results of the opened cover and the damaging effects to the near standing trees.

The overall mean tree height difference between the trees extracted from the UAV-CHM and ALS-CHM was 1.26m which indicate the overestimation of the tree height derived from UAV-CHM. The comparison of the UAV-CHM with ALS-CHM extracted tree height showed a correlation of 0.90 and coefficient of determination (R^2) of 0.81.The root mean square error (RMSE) was 2.1m, which is equivalent to 11% of the total height. The errors that lead to this overestimation of the upper canopy tree height extracted from UAV-CHM can be attributed to the following factors:

Point's cloudy density

The point cloud density generated from UAV image processing was high compared to LiDAR. In this study, the average density point cloud of 186 points/m^2 for UAV-DSM was estimated compared to the measured ALS points cloud of 6-8 points/m^2 as reported by Sadadi, (2016). The lower point density leads to underestimation of the tree height (Soonthornharuethai, 2016). Also, the software developer Agisoft, (2014) revealed that the software tends to produce extra dense point clouds, which are of almost the same density, if not denser, as LiDAR point clouds. The addition of the points clouds by the software during data processing results to high-density point cloud for UAV-DSM which may result in tree height value higher than the value obtained by ALS.

The difference period of data collection

The difference in time between LiDAR and UAV data collections may be the source of the tree height overestimates as a result of the sampled trees grew during the time. The LiDAR data was collected in 2013 while the current UAV images were collected in 2016 which is almost 3 years difference. The high tree growth rate was expected on the secondary forest where rehabilitation was conducted some years ago which can introduce more height variation between the two methods. The mean tree height difference of 5m was observed from plot 1 which was located in an area where trees have been planted more than 10 years ago. The dominant tree species on this plot was *Cinnamomum iners* which account for 50% of the sampled trees

in the plot located in the area where trees were planted especially plot 1. The study carried out by Affendy et al., (2009) to evaluate the growth rate of five indigenous timber species after 9 years of planting showed the range of height increment ranges between 0.77-1.38 m per year across the five species, with the *Cinnamomum iners* reported having a height increment of 0.77m per year. Based on the time difference between the two data sets tree growth can account for the difference in height.

Previous studies have shown a high correlation when the tree measurements by LiDAR system and tree height derived from CHM generated through a 3D image matching of UAV image compared. The study conducted by Vastaranta et al., (2013) shows a strong correlation when tree height derived from 3D aerial point clouds and ALS were compared with RMSE of 2.3m which is equivalent to 11.2% of the mean height. This result corresponds well with the results obtained in this study. Also, Ni et al., (2015) study revealed that the images taken by UAV could measure forest height at plot level with a coefficient of determination (R^2) of 0.87 and RMSE of 1.9 m when compared with ALS-CHM as reference data. This result is slightly more accurate than the results obtained by this study. A t-test revealed that there is a statistically significant difference between the tree height derived from 3D image matching of the UAV images and the tree height derived from LiDAR and ($P<0.05$) where the difference detected may be the result of the two factors mentioned above.

The estimated tree height by UAV-3D image matching is considered accurate when compared with the ALS tree height measurement. This attributed to the image taken with strong overlap (80% front and 60% side), which were useful for the generation of accurate DSM and the use of LiDAR DTM to generate CHM guarantee accurate measurements.

5.3. TLS data acquisition and Registration

The TLS data were acquired using TLS RIEGL VZ-400 and multiple scan approach was applied in this study as described in section 3.4.2. The registration of the scan was conducted based on registration using the corresponding tie points and the registration accuracy range from 0.019m and 0.038m with an average of 0.024m. The high registration depends on the number of tie points used for registration. In this study, 12-16 cylindrical retro-reflectors and 3-6 circular retro-reflectors were used depend on the level of occlusion within the plot which leads to the high accuracy registration of the scans. The high number and position of the tie point increase the registration accuracy (e.g. Plot 1, 10, 18, 28) also it has been revealed by (Madhibha, 2016).The source of error for the registration of the plots with high standard deviation is the occlusion where some of the reflectors been blocked by the trees within the plot to be viewed and scanned by TLS in a certain position. This decreases the number of tie point which affects the registration accuracy. This has been revealed by (Kankare, 2015, Madhibha, 2016) studies.

5.4. Individual Tree extraction and Parameters measurement

A total of 924 trees were measured in the field and 854 which is equivalent to 92.4% were extracted manually from the TLS point clouds, these results are comparable with Kankare, (2015) where trees extraction accuracy with multiple scans reported varied between 91.7–100%. A total of 70 trees equivalent to 7.6% of all trees measured in the field were missing from the trees extracted from TLS point cloud. This caused by the occlusion where a tree can be blocked by the undergrowth or another tree from being viewed by the scanner or the tree standing close to the scanner (less than 1.5m) where the scanner could not capture the tree. Also, some of the small trees were recorded missing as the result of the tree located far from the scanner. Therefore, the tree tag number could not be readable due to low point cloud density. Srinivasan et al., (2015) mentioned that the main problems associated with TLS technology are the inability to penetrate through the occluding undergrowth, leading to underestimations. The challenge of identifying the tree tag

number for some trees was resolved by overlaying the tree cloud points with the images taken by the digital camera mounted on TLS and specific tree and number were identified to guide tree extraction.

5.5. Comparison between Field and TLS measured tree height for lower canopy

The tree height was measured in the field using Leica DISTO 510 which use a laser technology. The laser pulse emitted by the instrument once hit the object it will record the information as a tree peak height. Measuring tree height in the tropical forest is unreliable because it is difficult to view the top canopy of the tree, especially for the upper canopy tree. The height derived from the TLS point cloud have been considered as a reference tree height for the lower canopy. The work by Calders et al., (2015) compared the tree height measured by a destructive method with the height measured by TLS and field height the TLS height agrees better with the reference height (destructive method) than the field measured height. This is because the TLS fires millions of laser pulses to capture the canopy while field measurements are normally based on a single measurement. Also, the experiment that was carried out at ITC before the field work demonstrated more accurate TLS measured height compared to the height measured with handheld instruments.

The comparison of field-measured tree height against TLS-derived tree height for lower canopy trees was conducted by performing the regression analysis. The results show a correlation (r) of 0.83 and coefficient of determination (R^2) of 0.69. The root mean square error (RMSE) was 1.4m which is equivalent to 15% of the total sampled tree height. This result shows also an overestimation of field height by 0.17m when the difference of the mean height of field and TLS measured height was calculated. These results are corresponding with the study carried by Hunter et al., (2013) that reported the error of field height measurements of individual trees ranged from 3 to 20% of total height. Other studies show the RMSE of the field tree height measurements ranged from 1.36 m to 4.29 m when compared with TLS measured tree height (Liang & Hyyppä, 2013) with the result obtained in this study tallies the minimum range.

Measuring tree height in the field required enough distance between the observer and the tree to increase the visibility of the tree tops which was a limited factor in tropical forest and results to overestimation or underestimation of tree height. Hunter et al., (2013) mention that, the offset between the measured distance and tree crown peak is because of insufficient distance between the observer and the tree. This would create difficulties to view the tree peak which is the sources of error for tree height measurement in the field (Figure 5-3).

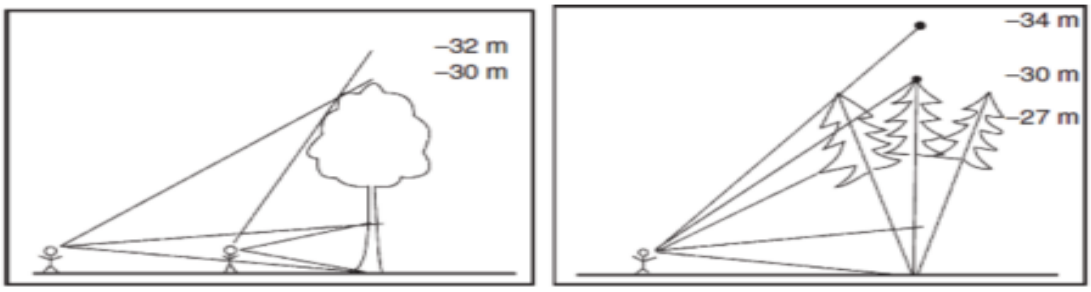

Source: Adopted from (Magar, 2014)

Figure 5-3: Error of field height measurement

The possible source of error for the tree height derived from TLS was the occlusion and overlapping of the tree crowns blocked the TLS pulse to reach the tree peak (Sadadi, 2016, Maas et al.,2008). In this study, the assumptions were these uncertainties were minimum for the lower canopy trees because the trees were

scanned from a different position under multiple scan approach. The trees were closer to the scanner compare to upper canopy trees and most of the understory were cleared.

5.6. Comparison between Field and TLS measured DBH for Upper and lower canopies

The DBH is very important input parameter for allometric equation used for estimating AGB/carbon stock. The DBH was measured in the field using diameter tape at the 1.3 meters above ground for the trees with DBH greater or equal to 10cm. The accuracy of measuring DBH in the field using a tape measure (DBH tape) can be affected by misallocation of a point (1.3m) of taking measurements, failing to place the tape in its proper level surface and misreading the tape divisions as well as the mistake of recording the measurements on the data sheet. These were some challenges noticed and minimized during field data collection, however, some of these factors have been revealed by the study of Weaver et al., (2015). In this study the Field DBH is the standard reference for validation of the TLS measured DBH. The TLS derived DBH was manually measured horizontally at 1.3m from the ground of the trees for all individual trees extracted from the TLS point cloud. The DBH was measured and recorded on Microsoft Excel sheet with corresponding tree tag number to match the field measurement for comparison.

The descriptive statistic result shows an underestimation of TLS DBH by 0.28 cm when taking the difference of the mean DBH of field and TLS measurements for 30 plots. The comparison of field measured DBH against TLS-derived DBH was conducted and regression analysis showed a high correlation (*r*) of 0.99, a coefficient of determination (R^2) of 0.986 and RMSE was 1.4 cm which is equivalent to 7% of the total DBH. Kankare et al., (2013) reported the RMSE of 1.48 cm for the DBH derived from the multiple scans TLS cloud points which are consistent with the results obtained in this study. Liang et al., (2016) revealed that, the accuracy of tree DBH derived from TLS data was demonstrated to be acceptable with an RMSE ranging between 1–2 cm and these estimates could be as accurate as those based on the national allometric models, therefore the RMSE of 1.4 cm achieved by this study is within the range. Other studies illustrated that the RMSE of the DBH estimation using the multiple scans method ranges between 0.90-1.90 cm (Liang, 2013, Maas et al., 2008). A t-test revealed that no statistically significant difference between the tree DBH derived from TLS point clouds and the tree DBH measured in the field ($P>0.05$), which correspond with the result obtained by Madhibha, (2016). These results obtained in this study and previous studies are demonstrating that TLS under multiple scans approach can be practically used for collecting forestry parameters in sample plots accurately for AGB/carbon stock estimation as long as the ground vegetation are cleared to minimize the occlusion for the tree trunk to be viewed properly by the scanner.

The measurement of DBH from the TLS point cloud produces biased when the tree stem form is not fully circular. Also, removal of unwanted understory vegetation point's clouds during data processing may result in the elimination of data points belonging to the stem lead to underestimation of tree DBH. These points were also mentioned in the study carried by Alberti et al., (2006). The technique of measuring the tree DBH from a different direction (Figure 5-4) and calculate the average can improve the accuracy of the trees that the stem form is not full circular. This was also explained in the study conducted by Saarinen et al., (2014). This technique was not applied in this study and may be the source of uncertainty obtained from the DBH derived from TLS point clouds.

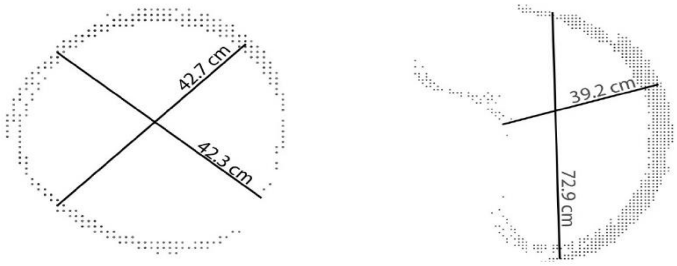

Figure 5-4: Stem form and measured DBH from TLS-point clouds from two different directions

Source: Adopted from Saarinen et al., (2014)

Some challenge on measuring the DBH from the TLS point cloud was experienced for trees branched together from the bottom caused some overlapping of the cloud points from one tree to another (Figure 5-5) and consume time while ensuring accurate measurement.

Figure 5-5: Example of trees branched together from the bottom

5.7. Aboveground Biomass for upper and lower Canopies

The upper and lower canopies AGB for each plot were calculated using the same allometric equation developed by Chave et al., (2014), which requires tree DBH, height and wood density as an input parameter (Equation 1-1). The species-specific wood density was used for most of the tree species while the trees with missing species-specific wood density (Appendix 8) the recommended average wood density of 0.57g/cm^3 for Asia region was applied (Aikawa et al., 2012, Schade & Ludwig, 2013).

The relationship for the upper and lower canopies AGB for the developed method and reference method was assessed separately. The estimated Field AGB, TLS AGB against Reference for lower canopy shows a very strong correlation of 0.98 and 0.99, the coefficient of determination (R^2) of 0.97 and 0.99, RMSE was 45.01Kg and 28.6Kg which is equivalent to 7% and 4.7% of the total observed lower canopy AGB for plots respectively. On the other hand, the coefficient of determination (R^2) of 0.98 and root mean square error (RMSE) of 524Kg which is equivalent to 7% of the total observed upper canopy AGB per plot for 30 plots was attained.

5.8. The overall AGB and carbon stock

The summation of the calculated AGB for upper and lower canopies provided an overall estimation of the total AGB for each plot (0.05ha). This was in line with the objective of this study that aimed to compare the estimated AGB of the developed method and reference on a plot based. Also, some of the comparable options to assess the effect of individual parameters on the AGB at plot level was developed and examined. The AGB for:

1. Developed method (TLS and UAV) was calculated using the TLS derived DBH, TLS derived height for the lower canopy and upper canopy tree height extracted from UAV-CHM.
2. Reference AGB was calculated using the field DBH, the ALS-CHM tree height for the upper canopy and TLS-derived tree height for the lower canopy.
3. TLS and ALS estimated AGB was calculated using the TLS DBH, TLS-derived tree height for the lower canopy and the ALS-CHM tree height for the upper canopy.
4. Field and ALS estimated AGB was calculated using the field DBH, field-measured tree height for the lower canopy and the ALS-CHM tree height for the upper canopy.

The descriptive statistics shows the estimated mean AGB for the developed method and reference was 8608.75 and 8425.44Kg per plot (0.05ha) respectively where the difference between these two means shows that the developed method got a higher value than the reference of 183.31 Kg per plot. The comparison of the overall estimated AGB for developed method against reference AGB showed a strong correlation of 0.99, the coefficient of determination (R^2) of 0.98 and a root mean square error (RMSE) was 536.25Kg per plot which is equivalent to 6.23% of the overall estimated AGB per plot for 30 plots. These results are equivalent to 168.51 and 172.2 t/ha for the reference and developed method respectively. The uncertainty of 6.23% obtained from this study is attributed to the uncertainty associated with the forestry input parameters for the allometric equation used to estimate the AGB. A t-test revealed that there is no statistically significant difference between the estimated AGB of the developed method and reference method on a plot based (The t-statistic < t-critical, P> 0.05). This indicates that the developed method can be used to estimate AGB with a reasonable accuracy.

Based on the comparison between developed method (TLS & UAV) and TLS and ALS estimated AGB demonstrated the effect of tree height extracted from UAV-CHM on AGB at the plot level. The results showed a strong correlation of 0.99, the coefficient of determination (R^2) of 0.99 and a root mean square error (RMSE) was 525.25Kg per plot which is equivalent to 6.10% of the overall estimated AGB per plot for 30 plots. The uncertainty of 6.10% obtained is accounted to the RMSE of 2.1m (11%) obtained for upper canopy tree height extracted from UAV-CHM when assessed. Also, the t-test showed there is a significance difference between the two means of tree height extracted from UAV-CHM and ALS-CHM. Previous study conducted by Hunter et al., (2013) revealed that, the uncertainty of individual tree ground-based height measurement ranges from 3 to 20% of the total height can lead to 5-6% uncertainty in overall AGB on plot base which corresponds with the uncertainty obtained by tree height extracted from UAV-CHM of 11% which resulted to inaccuracy of 6.1% to estimated AGB per plot for 30 plots.

However, the effect of the TLS derived DBH was assessed by comparing the AGB estimated using the TLS and ALS against the Referenced method. The results showed very high correlation 0.999 with R^2 of 0.99 and RMSE of 30Kg which is equivalent to 0.004% of estimated AGB at plot level. Saatchi et al., (2015) study reported that the DBH measurement with a bias of 0.19cm resulted to a negligible impact of less than 1% uncertainty to the overall biomass at plot level this is in line with the bias of 0.28cm and the RMSE of 0.004 obtained in this study (Table 4-20).

Developed method was compared with the Field and ALS estimated AGB to assess the uncertainty that can be obtained when field measured height for lower canopy AGB used as a reference. The results showed a strong correlation of 0.99, the coefficient of determination (R^2) of 0.988 and a root mean square error (RMSE) was 530.14Kg per plot which is equivalent to 6.16% of the overall estimated AGB per plot for 30 plots (Table 4-20). This indicates that the field-measured tree height for lower canopy can be reliable for lower canopy AGB estimation as the attained uncertainty close to 6.23% obtained when the accurate tree height derived from TLS data used as a reference at the plot level.

A total carbon stock per plot (0.05ha) was calculated (Equation 3-2) by multiplying a total AGB per plot with the conversion factor of 0.47 and represented in megagrams (Mg). The descriptive statistics shows the estimated mean carbon stock for the developed method (TLS & UAV) and reference method (field and ALS) was 4.05 and 3.97Mg per plot respectively where the difference between these two means shows that the developed method achieved a higher value of carbon stock of 0.08Mg per plot. This result is equivalent to 80.92 and 79.20Mg/ha of carbon stock estimated by the developed method and reference method respectively. The developed method acquired 1.72Mg/ha higher value of carbon stock compared to reference method based on the mean difference between the two methods, which is equivalent to 2% of the mean carbon stock per hectare.

5.9. Limitation

The GPS error was a limitation, especially locating the plot center and matching the tree location from the field and the ortho-mosaic and CHM.

The GCPs' placement in the ground in a tropical forest is quite challenging because of the close canopy. Therefore, the UAV images were acquired on the edge of the forest were open spaces for GCPs" placements were available.

The rotors UAV system cover a small area and are the recommended UAV system for the tropical forest because of its ability to take off vertically compare to fix wing UAV system which covers a wide area but take off horizontal which require enough space which is limited in a tropical forest.

The difference in time of data collection between the LiDAR and the UAV flight may be the source of the difference in height as a result of the sampled trees grew during the time.

6. CONCLUSIONS AND RECOMMENDATIONS

6.1. Conclusion

This study examines the performance of integrated TLS information and upper canopy tree heights from CHM generated from 3D image matching of UAV imagery to estimate AGB/carbon stock of vertical complex structured tropical rain-forest. The allometric equation input forestry parameters (DBH and tree height) for AGB/carbon stock estimation were assessed.

The upper canopy tree height extracted from CHM generated from 3D image matching of UAV imagery was assessed by comparing with ALS Canopy Height Model. The attained R^2 and RMSE values for the upper canopy height for the 30 plots are 0.81 and 2.1m (11%) respectively. The lower canopy tree height measured in the field was compared to tree height derived from TLS point cloud. The achieved R^2 and RMSE values for the upper canopy height for the 30 plots are 0.69 and 1.4m (15%) respectively. The accuracy of upper and lower canopy tree DBH measured by TLS was compared to DBH measured in the field and the achieved R^2 and RMSE values for the upper canopy height for the 30 plots are 0.98 and 1.48cm (8%) respectively.

The assessed forest parameters were applied to the generic allometric equation to estimate the upper and lower canopies AGB separately. The overall AGB per plot was calculated by combining the upper and lower canopies estimated AGB for each plot. The overall AGB on a plot based estimated by the developed method was assessed by comparing with the reference AGB. The achieved R^2 and RMSE values for the overall AGB per plot for the 30 plots were 0.98 and 536.25 Kg per plot (6.23%) respectively. A t-test revealed that there is no statistically significant difference between the estimated AGB of the developed method and reference on a plot based ($P>0.05$). This indicates the integration of TLS information and CHM derived from the UAV images give an opportunity for accurately estimation of the AGB of vertical complex structured tropical rain-forest.

The novel of this study presents a strong advantage in the implementation of REDD+ and it's MRVs' system because it requires an accurate and cost effective method for estimation of AGB and regular monitoring over certain time frames. A UAV may contribute to a dramatic cost reduction of repeated monitoring of tropical forests by replacing the LiDAR for upper canopy tree height estimation. However, once a LiDAR DTM is used and the DSM generated from images acquired by UAV with strong overlap condition, reasonable accuracy for AGB estimation is guaranteed. On the other hand, these results demonstrated that TLS under multiple scans approach can be practically used for collecting forestry parameters (DBH and lower canopy tree height) in sample plots accurately for AGB and carbon stock estimation as long as the ground vegetation are cleared to minimize the occlusion for the tree trunk to be viewed properly by the TLS scanner.

The following are the answers to the research questions of this study:

How accurate is the upper canopy tree height derived from CHM developed using 3D image matching of UAV imagery compared to ALS Canopy Height Model?

The accuracy of the upper canopy tree height derived from UAV-CHM upon comparing with the tree height derived from ALS-CHM achieved an R^2 of 0.81 and RMSE of 2.1m (11%).This means 89% of the tree height was accurately estimated by the canopy height model developed using the DSM generated from 3D image matching of UAV imagery and the LiDAR DTM. Therefore, the null hypothesis was rejected.

How accurate is the lower canopy tree height measured in the field compare to tree height derived from TLS data?

The accuracy of the lower canopy tree height measured in the field when compared to tree height derived from TLS point clouds achieved an R^2 of 0.69 and RMSE of 1.4m (15%). This means that 85% of the tree height was accurately measured by Leica DISTO 510 in the field. Hence, the null hypothesis was rejected which state that the accuracy will be <80%.

How accurate is the DBH derived from TLS data compare to field measurement?

The accuracy of the DBH derived from TLS point clouds when compared to field measured DBH achieved an R^2 of 0.986 and RMSE of 1.4cm (7%). This means the 93% of the DBH was accurately measured from the TLS point cloud. Hence the null hypothesis was rejected.

How accurate is forest AGB/carbon stock on plot base estimated by developed method (TLS DBH+TLS lower canopy height + upper canopy UAV height) compared to the reference method (Field DBH + Field lower canopy height + ALS upper canopy height)?

The accuracy of the forest AGB/carbon stock on plot base estimated by the developed method when compared to reference method achieved an R^2 of 0.98 and RMSE of 536.25 Kg per plot (6.23%). This means the 93.77% of the AGB/carbon stock was accurately estimated by integrating TLS information and upper canopy tree heights from Canopy height model generated from 3D image matching of UAV imagery. Hence, the null hypothesis was rejected.

6.2. Recommendations

The more accurate GPS particularly a Differential GPS is required to record the plot center to make the tree matching process much easier and accurate.

More investment required to be able to place GCPs' in the dense forest areas rather than depend only on the edge of the forest.

Assess the effects of terrain variation on the quality of DSM generated from the 3D image matching of the UAV image.

LIST OF REFERENCES

Affendy, H., Aminuddin, M., Razak, W., Arifin, A., & Mojiol, A. R. (2009). Growth increments of indigenous species planted in the secondary forest area. *Research Journal of Forestry*, *3*(1), 23–28. doi.org/10.3923/rjf.2009.23.28

Agisoft. (2014). *Orthophoto and DEM generation with Agisoft PhotoScan Pro 1.1 (with ground controls points):Tutorial (beginner level)* (Vol. 1).

Aicardi, I., Dabove, P., Lingua, A., & Piras, M. (2016). Integration between TLS and UAV photogrammetry techniques for forestry applications. *iForest - Biogeosciences and Forestry*, *9*, 1–7. doi.org/10.3832/ifor1780-009

Aikawa, S., Akahori, S., Awaya, Y., Ehara, M., Hirata, Y., Furuya, N., … Yokota, Y. (2012). *REDD+ Cookbook 1-How To Measure And Monitor Forest Carbon*. *Forestry and Forest Products Research Institute (FFPRI)*. Ibaraki, Japan. Retrieved from http://www.ffpri.affrc.go.jp/redd-rdc/en/reference/cookbook.html

Alberti, G., Marelli, A., Piovesana, D., Peressotti, A., Zerbi, G., Gottardo, E., & Bidese, F. (2006). Carbon stocks and productivity in forest plantations (Kyoto forests) in Friuli Venezia Giulia (Italy). *Forest@ - Rivista Di Selvicoltura Ed Ecologia Forestale*, *3*(4), 488–495. doi.org/10.3832/efor0414-0030488

Anderson, K., & Gaston, K. J. (2013). Lightweight unmanned aerial vehicles will revolutionize spatial ecology. *Frontiers in Ecology and the Environment*, *11*(3), 138–146. doi.org/10.1890/120150

Angelsen, A., Brockhaus, M., Sunderlin, W. D., & Verchot, L. V. (Eds). (2012). *Analysing REDD+: Challenges and choices*. Bogor, Indonesia: Center for International Forestry Research (CIFOR). doi.org/10.17528/cifor/003805

Basuki, T. M., van Laake, P. E., Skidmore, A. K., & Hussin, Y. A. (2009). Allometric equations for estimating the above-ground biomass in tropical lowland Dipterocarp forests. *Forest Ecology and Management*, *257*(8), 1684–1694. doi.org/10.1016/j.foreco.2009.01.027

Bienert, A., Scheller, S., Keane, E., Mullooly, G., & Mohan, F. (2006). Application of Terrestrial Laser Scanners For The Determination Of Forest Inventory Parameters. *International Archives of Photogrammetry , Remote Sensing and Spatial Information Science*, *36*, 5. doi.org/10.1111/jam.12647

Bottcher, H., Eisbrenner, K., Fritz, S., Kindermann, G., Kraxner, F., McCallum, I., & Obersteiner, M. (2009). An assessment of monitoring requirements and costs of "Reduced Emissions from Deforestation and Degradation." *Carbon Balance and Management*, *4*, 7. doi.org/10.1186/1750-0680-4-7

Brown. (2002). Measuring carbon in forests: Current status and future challenges. *Environmental Pollution*, *116*(3), 363–372. doi.org/10.1016/S0269-7491(01)00212-3

Brown, S. (1997). Estimating biomass and biomass change of tropical forests: a primer. Retrieved August 14, 2016, from http://www.fao.org/docrep/W4095E/W4095E00.htm

Calders, K., Newnham, G., Burt, A., Murphy, S., Raumonen, P., Herold, M.,Kaasalainen, M. (2015). Nondestructive estimates of above-ground biomass using terrestrial laser scanning. *Methods in Ecology and Evolution*, *6*(2), 198–208. doi.org/10.1111/2041-210X.12301

Chave, J., Rejou-Mechain, M., Burquez, A., Chidumayo, E., Colgan, M. S., Delitti, W. B. C., … Vieilledent, G. (2014). Improved allometric models to estimate the aboveground biomass of tropical trees. *Global Change Biology*, *20*(10), 3177–3190. doi.org/10.1111/gcb.12629

Christopher L. Heffner. (n.d.). Chapter 8.3 Types of Distributions | AllPsych. Retrieved January 4, 2017, from http://allpsych.com/researchmethods/distributions/

Curtis, P. S. (2008). Estimating aboveground carbon in live and standing dead trees. In C. M. Hoover (Ed.), *Field Measurements for Forest Carbon Monitoring: A Landscape-Scale Approach* (pp. 39–44). Durham,

USA: Springer.

FAO. (2010). *Global Forest Resources Assessment 2010*. *America* (Vol. 163). Rome, Italy. Retrieved from http://www.fao.org/docrep/013/i1757e/i1757e.pdf

Getzin, S., Wiegand, K., & Schoning, I. (2012). Assessing biodiversity in forests using very high-resolution images and unmanned aerial vehicles. *Methods in Ecology and Evolution*, *3*(2), 397–404. doi.org/10.1111/j.2041-210X.2011.00158.x

Gibbs, H. K., Brown, S., Niles, J. O., & Foley, J. A. (2007). Monitoring and estimating tropical forest carbon stocks: making REDD a reality. *Environmental Research Letters*, *2*, 1–13. doi.org/10.1088/1748-9326/2/4/045023

Gomez, C., Hayakawa, Y., & Obanawa, H. (2015). A study of Japanese landscapes using structure from motion derived DSMs and DEMs based on historical aerial photographs: New opportunities for vegetation monitoring and diachronic geomorphology. *Geomorphology*, *242*, 11–20. doi.org/10.1016/j.geomorph.2015.02.021

Hasmadi, I., Amirin Khairul, M., & Hidayah Siti Noor, A. . (2008). Estimated DEM uncertainty in creating a 3-D of the UPM's Ayer Hitam Forest reserve in Selangor, Malaysia. *Geografia - Malaysian Journal of Society and Space*, *4*(1), 45–53. Retrieved from http://www.ukm.my/geografia

Hunter, M. O., Keller, M., Victoria, D., & Morton, D. C. (2013). Tree height and tropical forest biomass estimation. *Biogeosciences*, *10*(12), 8385–8399. doi.org/10.5194/bg-10-8385-2013

Hunter, M. O., Keller, M., Vitoria, D., & Morton, D. C. (2013). Geoscientific Instrumentation Methods and Data Systems Tree height and tropical forest biomass estimation. *Biogeosciences Discuss*, *10*(6), 10491–10529. doi.org/10.5194/bgd-10-10491-2013

IPCC. (1996). Task Force on National Greenhouse Gas Inventories. Retrieved February 11, 2017, from http://www.ipcc-nggip.iges.or.jp/public/2006gl/vol4.html

Kahyani, S., Hosseini, S., & Basiri, R. (2011). The Basic of Analytical of Simple Linear Regression in Forestry Studies (Case Study: Relationship Between Basal Area and Tree Coverage of Quercus brantii Lindl. In Absardeh, Chahar Mahale and Bakhtiari). *World Applied Sciences Journal*, *14*(10), 1599–1606.

Kankare, V. (2015). The prediction of single-tree biomass, logging recoveries and quality attributes with laser scanning techniques. *Dissertationes Forestales*, 1. doi.org/10.14214/df.195

Kankare, V., Holopainen, M., Vastaranta, M., Puttonen, E., Yu, X., Hyypp, J.,Alho, P. (2013). Individual tree biomass estimation using terrestrial laser scanning. *ISPRS Journal of Photogrammetry and Remote Sensing*, *75*, 64–75. doi.org/10.1016/j.isprsjprs.2012.10.003

Karna, Y. K. (2012). *Mapping Above Ground Carbon Using WorldView Satellite Image And Lidar Data In Relationship With Tree Diversity Of Forests.* MSc thesis,University of Twente Faculity of Geo-information and Earth Observation Science (ITC). Enschede,The Netherlands. Retrieved from http://www.itc.nl/library/papers_2016/msc/nrm/karna.pdf

Koh, L. P., & Wich, S. A. (2012). Dawn of drone ecology: low-cost autonomous aerial vehicles for conservation. *Tropical Conservation Science*, *5*(2), 121–132. doi.org/WOS:000310846600002

Lawas, C. J. C. (2016). *Complementary use of Airborne Lidar and Terrestrial Laser Scanner to Assess Above Ground Biomass / Carbon in Ayer Hitam tropical rain forest reserve*. MSc thesis,University of Twente Faculity of Geo-information and Earth Observation Science (ITC). Enschede,The Netherlands. Retrieved from http://www.itc.nl/library/papers_2016/msc/nrm/lawas.pdf

Leon, J. X., Roelfsema, C. M., Saunders, M. I., & Phinn, S. R. (2015). Measuring coral reef terrain roughness using "Structure-from-Motion" close-range photogrammetry. *Geomorphology*, *242*, 21–28. doi.org/10.1016/j.geomorph.2015.01.030

Lepun, P., Faridah, H. I., & Jusoff, K. (2007). Tree species distribution in Ayer Hitam Forest Reserve, Selangor, Malaysia. In *EEESD 07 Proceedings of the 3rd IASMEWSEAS International Conference on Energy Environment Ecosystems and Sustainable Development* (pp. 75–81). Agios Nikolaos, Greece. Retrieved from https://www.researchgate.net/publication/266485744

Liang, X. (2013). *Feasibility of Terrestrial Laser Scanning for Plotwise Forest Inventories*. *Publications of the Finnish Geodetic Institute* (Vol. 149).

Liang, X., & Hyyppä, J. (2013). Automatic stem mapping by merging several terrestrial laser scans at the feature and decision levels. *Sensors (Switzerland)*, *13*(2), 1614–1634. doi.org/10.3390/s130201614

Liang, X., Kankare, V., Hyyppa, J., Wang, Y., Kukko, A., Haggrén, H., Vastaranta, M. (2016). Terrestrial laser scanning in forest inventories. *ISPRS Journal of Photogrammetry and Remote Sensing*, *115*, 63–77. doi.org/10.1016/j.isprsjprs.2016.01.006

Lisein, J. (2012). Creation of a Canopy Height Model from mini-UAV Imagery (Poster), *257*(3). Retrieved from http://orbi.ulg.ac.be/bitstream/2268/129781/1/ModeleNumCanopee_drone_poster.pdf

Lisein, J., Pierrot-Deseilligny, M., Bonnet, S., & Lejeune, P. (2013). A photogrammetric workflow for the creation of a forest canopy height model from small unmanned aerial system imagery. *Forests*, *4*(4), 922–944. doi.org/10.3390/f4040922

Maas, H.-G., Bienert, A., Scheller, S., & Keane, E. (2008). Automatic Forest Inventory Parameter Determination from Terrestrial Laser Scanner Data. *International Journal of Remote Sensing*, *29*(5), 1579–1593. doi.org/10.1080/01431160701736406

Madhibha, T. P. (2016). *Assessment of Above Ground Biomass with Terrestrial Lidar using 3D Quantitative Structure Modelling in Tropical Rain Forest of Ayer Hitam Forest Reserve,Malaysia*. MSc thesis,University of Twente Faculity of Geo-information and Earth Observation Science (ITC). Enschede,The Netherlands. Retrieved from http://www.itc.nl/library/papers_2016/msc/nrm/madhibha.pdf

Magar, A. T. (2014). *Estimation and mapping of forest biomass and carbon using point-clouds derived from airborne LiDAR and from 3D photogrammetric matching of aerial images*. MSc thesis,University of Twente Faculity of Geo-information and Earth Observation Science (ITC). Enschede,The Netherlands. Retrieved from http://www.itc.nl/library/papers_2014/msc/gem/thapamagar.pdf

Mohren, G., Hasenauer, H., Köhl, M., & Nabuurs, G.-J. (2012). Forest inventories for carbon change assessments. *Current Opinion in Environmental Sustainability*, *4*(6), 686–695. doi.org/10.1016/j.cosust.2012.10.002

Newnham, G. J., Armston, J. D., Calders, K., Disney, M. I., Lovell, J. L., Schaaf, C. B.,Danson, F. M. (2015). Terrestrial Laser Scanning for Plot-Scale Forest Measurement. *Current Forestry Reports*, *1*(4), 239–251. doi.org/10.1007/s40725-015-0025-5

Ni, W., Liu, J., Zhang, Z., Sun, G., & Yang, A. (2015). Evaluation of UAV-based Forest Inventory System Compared with Lidar Data. In *IEEE INTERNATIONAL GEOSCIENCE AND REMOTE SENSING SYMPOSIUM (IGARSS)* (pp. 3874–3877). IEEE, 345 E 47TH ST, NEW YORK, NY 10017 USA. doi.org/10.1109/IGARSS.2015.7326670

Nurul-Shida, N., Hanum, F., W.M, W. R., & K, K. (2014). Community Structure of Trees in Ayer Hitam Forest Reserve , Puchong ,. *The Malaysian Forester*, *77*(1), 73–86. Retrieved from https://www.researchgate.net/publication/270106458

Ota, T., Ogawa, M., Shimizu, K., Kajisa, T., Mizoue, N., Yoshida, S., Ket, N. (2015). Aboveground biomass estimation using structure from motion approach with aerial photographs in a seasonal tropical forest. *Forests*, *6*(11), 3882–3898. doi.org/10.3390/f6113882

Palace, M., Sullivan, F. B., Ducey, M., & Herrick, C. (2016). Estimating Tropical Forest Structure Using a Terrestrial Lidar. *Plos One*, *11*(4), 1–19. doi.org/10.1371/journal.pone.0154115

Paneque-Gálvez, J., McCall, M., Napoletano, B., Wich, S., & Koh, L. (2014). Small Drones for Community-Based Forest Monitoring: An Assessment of Their Feasibility and Potential in Tropical Areas. *Forests*, *5*(6), 1481–1507. doi.org/10.3390/f5061481

Patenaude, G., Hill, R. A., Milne, R., Gaveau, D. L. A., Briggs, B. B. J., & Dawson, T. P. (2004). Quantifying forest above ground carbon content using LiDAR remote sensing. *Remote Sensing of Environment*, *93*(3), 368–380. doi.org/10.1016/j.rse.2004.07.016

Picard, N., Saint-Andre, L., & Henry, M. (2012). *Manual for building tree volume and biomass allometric equations: from field measurement to prediction. Vasa*. Rome, Italy: FAO. doi.org/10.1073/pnas.0703993104

Ritter, B. (2014). *Use of unmanned aerial vehicles (UAV) for urban tree inventories*. *All Theses*. Msc thesis, Clemson University. Retrieved from http://tigerprints.clemson.edu/all_theses

Saarinen, N., Vastaranta, M., Kankare, V., Tanhuanpää, T., Holopainen, M., Hyyppä, J., & Hyyppä, H. (2014). Urban-tree-attribute update using multisource single-tree inventory. *Forests*, *5*(5), 1032–1052. doi.org/10.3390/f5051032

Saatchi, S., Meyer, V., Yang, Y., Fricker, A., & Yu, Y. (2015). Uncertainty of Carbon Estimates. *United States Agency for International Development*.

Sadadi, O. (2016). *Accuracy of Measuring Tree Height Using Airborne Lidar and Terrestrial Laser Scanner and Its Effect on Estimating Forest Biomass and Carbon Stock in Ayer Hitam Tropical Rain Forest Reserve , Malaysia*. MSc thesis,University of Twente Faculity of Geo-information and Earth Observation Science. Enschede,The Netherlands. Retrieved from http://www.itc.nl/library/papers_2016/msc/nrm/ojoatre.pdf

Schade, J., & Ludwig, R. (2013). Forest carbon baseline study in Leyte As a federally owned enterprise, GIZ supports the German Government in achieving its objectives in the field of international cooperation for sustainable development. Retrieved from http://www.faspselib.denr.gov.ph/Forest%20Carbon%20Baseline%20Study%20in%20Leyte.pdf

Sherali, H. D., Narayanan, A., & Sivanandan, R. (2003). Estimation of origin-destination trip-tables based on a partial set of traffic link volumes. *Transportation Research Part B: Methodological*, *37*(9), 815–836. doi.org/10.1016/S0191-2615(02)00073-5

Soonthornharuethai, P. (2016). *Comparing 3D Point Clouds from Image-based Matching Method and Airborne LiDAR in Tropical Rainforest Reserve of Ayer Hitam, Malaysia.* MSc thesis,University of Twente Faculity of Geo-information and Earth Observation Science (ITC). Enschede,The Netherlands. Retrieved from http://www.itc.nl/library/papers_2016/msc/nrm/Phanintra.pdf

Srinivasan, S., Popescu, S. C., Eriksson, M., Sheridan, R. D., & Ku, N. W. (2014). Multi-temporal terrestrial laser scanning for modeling tree biomass change. *Forest Ecology and Management*, *318*, 304–317. doi.org/10.1016/j.foreco.2014.01.038

Srinivasan, S., Popescu, S. C., Eriksson, M., Sheridan, R. D., & Ku, N. W. (2015). Terrestrial laser scanning as an effective tool to retrieve tree level height, crown width, and stem diameter. *Remote Sensing*, *7*(2), 1877–1896. doi.org/10.3390/rs70201877

Tesfai, S. (2015). *Upscaling Estimation of Tropical Rain Forest Biomass / Carbon Stock Using TLS and Landsat-8 ETM + Data*. University of Twente Faculity of Geo-information and Earth Observation Science. Retrieved from https://ezproxy.utwente.nl:2315/library/2015/msc/nrm/tesfai.pdf

Turner, D., Lucieer, A., & Watson, C. (2012). An Automated Technique for Generating Georectified Mosaics from Ultra-High Resolution Unmanned Aerial Vehicle (UAV) Imagery , Based on Structure from Motion (SfM) Point Clouds. *Remote Sensing*, *4*, 1392–1410. doi.org/10.3390/rs4051392

UNAVOC. (2013). Riegl TLS Field Operation Manual and Workflow, *400*.

Uramoto, Y., Zhu, L., Tachibana, K., Shimamura, H., & Ogaya, N. (2012). Development of Photogrammetry System for Grasping Forest Resources Information. In *XXII ISPRS CONGRESS, TECHNICAL COMMISSION VIII* (Vol. 39-B8, pp. 447–450). doi.org/10.5194/isprsarchives-XXXIX-B8-447-2012

Vashum, K. T., Jayakumar, S., & T. Vashum, K. (2012). Methods to Estimate Above-Ground Biomass and Carbon Stock in Natural Forests - A Review. *Journal of Ecosystem & Ecography*, *2*(4), 100–116. doi.org/10.4172/2157-7625.1000116

Vastaranta, M., Wulder, M. A., White, J. C., Pekkarinen, A., Tuominen, S., Ginzler, C., Hyyppa, H. (2013). Airborne laser scanning and digital stereo imagery measures of forest structure: comparative results and implications to forest mapping and inventory update. *Canadian Journal of Remote Sensing*, *39*(5), 382–395. doi.org/10.5589/m13-046

Wang, C., & Glenn, N. F. (2008). A linear regression method for tree canopy height estimation using airborne lidar data. *Canadian Journal of Remote Sensing*, *34*(Supplement 2), s217–s227. doi.org/10.5589/m08-043

Weaver, S. A., Ucar, Z., Bettinger, P., Merry, K., Faw, K., & Cieszewski, C. J. (2015). Assessing the accuracy of tree diameter measurements collected at a distance. *Croatian Journal of Forest Engineering*, *36*(1), 73–84. Retrieved from http://www.engineeringvillage.com/blog/document.url?mid=geo_a29da0d14c57a23b43M753d1017816338&database=geo

Wezyk, P., Kozioł, K., Glista, M., & Pierzchalski, M. (2007). Terrestrial laser scanning versus traditional forest inventory first results from the polish forests. *ISPRS Workshop on Laser Scanning 2007 and SilviLaser 2007, Finland*, *36*(3), 424–429. Retrieved from http://www.isprs.org/proceedings/XXXVI/3-W52/final_papers/Wezyk_2007.pdf

Zaki, N. A., & Latif, Z. A. (2016). Carbon Sinks and Tropical Forest Biomass Estimation: A Review on Role of Remote Sensing In Aboveground-Biomass Modelling. *Geocarto International*, *6049*(4), 1–41. doi.org/10.1080/10106049.2016.1178814

Zheng, L., Yu, M., Song, M., Stefanidis, A., Ji, Z., & Yang, C. (2016). Registration of Long-Strip Terrestrial Laser Scanning Point Clouds Using RANSAC and Closed Constraint Adjustment. *Remote Sensing*, *8*(4), 278. doi.org/10.3390/rs8040278

APPENDICES

Appendix 1: Distribution curves of field and TLS measured DBH

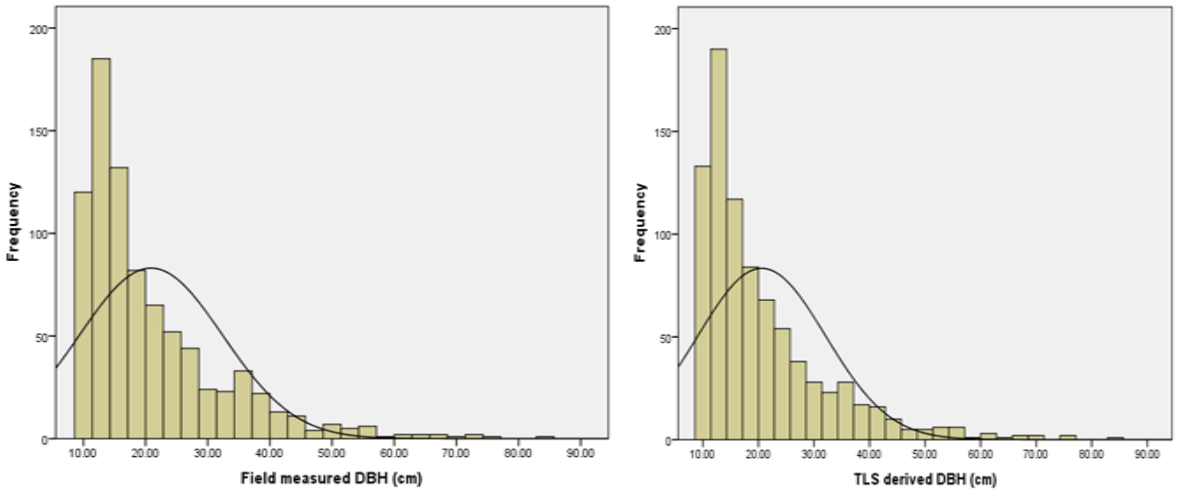

Appendix 2: Distribution curves of field and TLS measured lower canopy tree height

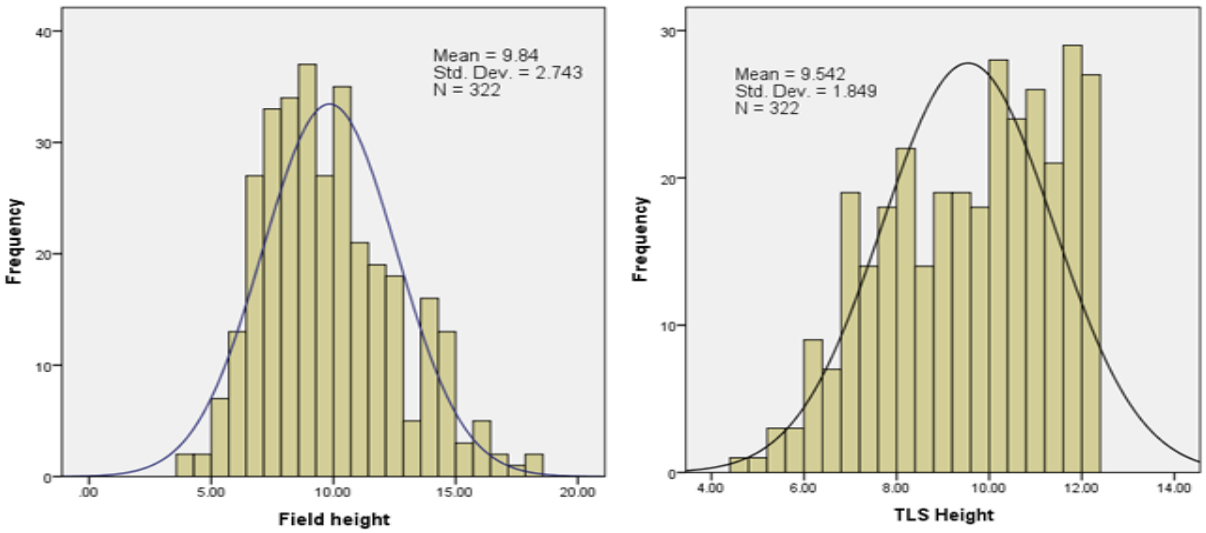

Appendix 3: Distribution curves of UAV and ALS extracted Upper canopy tree height

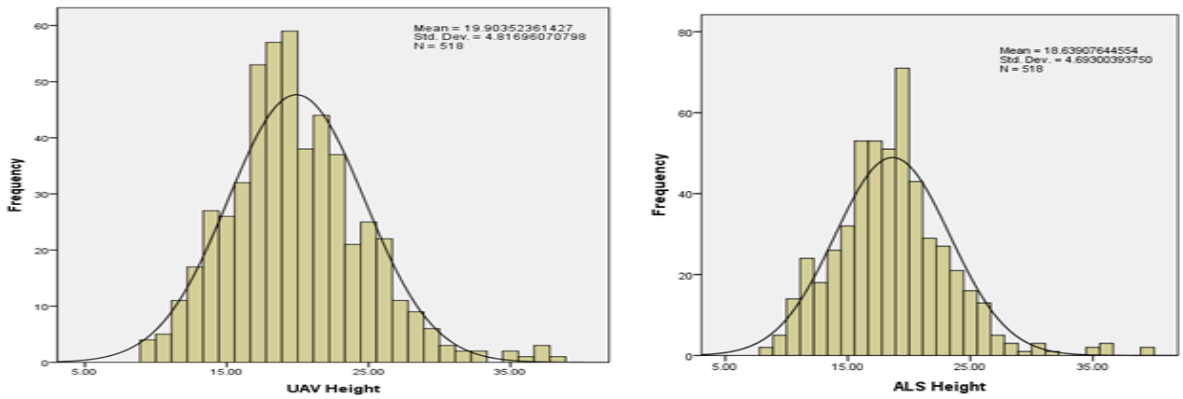

Appendix 4: Distribution curves of observed and reference AGB on plot base

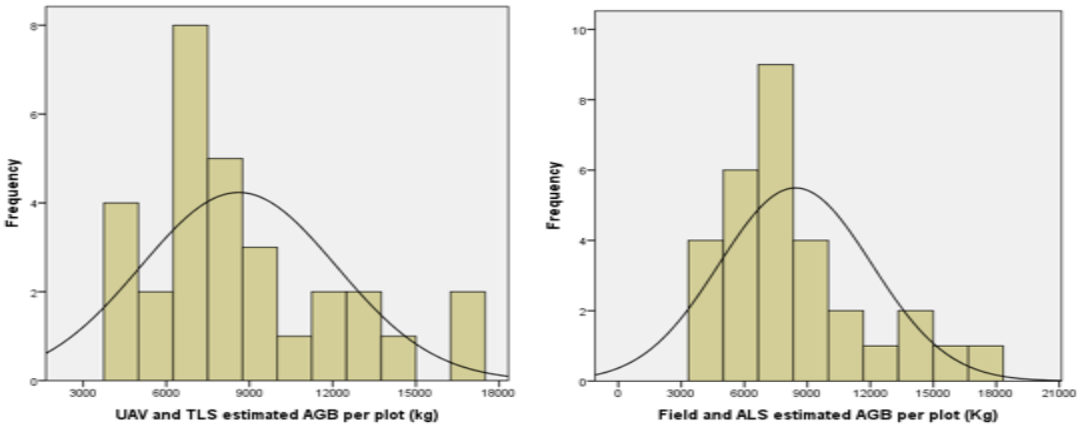

Appendix 5: The mean height and mean height difference per plot for upper canopy trees

Plot No.	1	2	3	4	5	6	7	8	9	10
UAV-CHM mean height(m)	19.3	18.9	18.96	25.5	23.29	24.49	23.95	19.11	22.25	21
ALS-CHM mean height(m)	14.9	17.91	17.94	23.37	21.57	21.99	22.68	17.43	20.95	19.05
Mean height difference(m)	4	1	1	2	2	3	1	2	1	2
Plot No.	11	12	13	14	15	16	17	18	19	20
UAV-CHM mean height(m)	16.8	20.55	16.64	18.86	17.9	17.83	25.22	20.33	19.06	23.71
ALS-CHM mean height(m)	17.48	19.26	16.22	18.15	18.91	18	23.76	21.77	17.8	21.69
Mean height difference(m)	-1	1	0	1	-1	0	1	-1	1	2
Plot No.	21	22	23	24	25	26	27	28	29	30
UAV-CHM mean height(m)	20.11	21.43	22.76	20.27	22.07	15.58	14.43	15.72	15.46	19.9
ALS-CHM mean height(m)	19.1	19.19	20.43	19.5	20.17	14.12	13.86	14.62	13.69	19.38
Mean height difference(m)	1	2	2	1	2	1	1	1	2	1

Appendix 6: Slope correction table

Slope (%)	Radius (m)	Slope (%)	Radius (m)	Slope (%)	Radius (m)
0	12.62				
1	12.62	36	13.01	71	13.97
2	12.62	37	13.03	72	14.00
3	12.62	38	13.05	73	14.04
4	12.62	39	13.07	74	14.07
5	12.62	40	13.09	75	14.10
6	12.63	41	13.12	76	14.14
7	12.63	42	13.14	77	14.17
8	12.64	43	13.16	78	14.21
9	12.64	44	13.19	79	14.24
10	12.65	45	13.21	80	14.28
11	12.65	46	13.24	81	14.31
12	12.66	47	13.26	82	14.35
13	12.67	48	13.29	83	14.38
14	12.68	49	13.31	84	14.42
15	12.69	50	13.34	85	14.45
16	12.70	51	13.37	86	14.49
17	12.71	52	13.39	87	14.52
18	12.72	53	13.42	88	14.56
19	12.73	54	13.45	89	14.60
20	12.74	55	13.48	90	14.63
21	12.75	56	13.51	91	14.67
22	12.77	57	13.53	92	14.71
23	12.78	58	13.56	93	14.74
24	12.79	59	13.59	94	14.78
25	12.81	60	13.62	95	14.82
26	12.82	61	13.65	96	14.85
27	12.84	62	13.68	97	14.89
28	12.86	63	13.72	98	14.93
29	12.87	64	13.75	99	14.97
30	12.89	65	13.78	100	15.00
31	12.91	66	13.81	101	15.04
32	12.93	67	13.84	102	15.08
33	12.95	68	13.87	103	15.12
34	12.97	69	13.91	104	15.15
35	12.99	70	13.94	105	15.19

Appendix 7: Data collection sheet

Author:		**Sample:** **Slope (%):**		**Plot radius: 12.6**		**Data:**	**Ayer Hitam, 2016**	
GPS Plot		Latitude: Longitude:					Crown diam. (m)	Crown cover (%)
ID	Tree No.	Latitude	Longitude	Species	DBH (cm)	Field height (m)		

Appendix 8: List of Tree Species Wood Density

ID	*Species*	Wood_Den_g.-cm3	ID	*Species*	Wood_Den_g.-cm3
1	*Acacia mangium*	0.507	85	*Dillenia suffruticosa*	0.623
2	*Actinodaphne sesquipedalis*	0.510	86	*Diospyros spp*	0.667
3	*Adenanthera malayana*	0.720	87	*Diplospora malaccensis*	0.570
4	*Aglaia acariaeantha*	0.672	88	*Dipterocarpus baudii*	0.745
5	*Aidia densiflora*	0.680	89	*Dipterocarpus crinitus*	0.745
6	*Alstonia spp*	0.570	90	*Dipterocarpus verrucosus*	0.673
7	*Anisophyllea griffithii*	0.840	91	*Dyera costulata*	0.338
8	*Antidesma caspidatum*	0.800	92	*Elaeis guineensis*	0.570
9	*Aporosa symplocoides*	0.615	93	*Elaeocarpus ganitrus*	0.484
10	*Aquilaria malaccensis*	0.320	94	*Elaeocarpus mastersii*	0.484
11	*Archidendron pauciflorum*	0.570	95	*Elaeocarpus petiolatus*	0.484
12	*Arena obtusifolia*	0.570	96	*Elateriospermum tapos*	0.693
13	*Argania spinosa*	0.570	97	*Endospermum diadenum*	0.367
14	*Arthrophyllum diversifolium*	0.550	98	*Eugenia grandis*	0.650
15	*Artocarpus elasticus*	0.363	99	*Ficus spp*	0.399
16	*Artocarpus gomezianus*	0.540	100	*Gaham badak*	0.570
17	*Artocarpus interger*	0.483	101	*Garcinia nervosa*	0.450
18	*Artocarpus rigidus*	0.513	102	*Gardenia tubifera*	0.670
19	*Artocarpus scortechinii*	0.440	103	*Gironniera nervosa*	0.450
20	*Atrocarpus odoratissimus*	0.483	104	*Gluta renghas*	0.573
21	*Azadirachta excelsa*	0.480	105	*Gonystylus affinis*	0.546
22	*Baccaurea griffithii*	0.624	106	*Guttiferaeand lauraceae*	0.570
23	*Beilschmiedia madang*	0.500	107	*Gymnacranthera bancana*	0.540
24	*Bridelia tomentosa*	0.665	108	*Gynotroches axillaris*	0.520
25	*Callerya atropurpurea*	0.560	109	*Heritiera javanica*	0.686
26	*Calophyllum biflorum*	0.560	110	*Hopea odorata*	0.635
27	*Calophyllum javanicum*	0.550	111	*Horsfieldia spp*	0.635
28	*Campnosperma auriculatum*	0.356	112	*Ilex cymosa*	0.490
29	*Canarium apertum*	0.500	113	*Ixonanthes icosandra*	0.696
30	*Canarium granddifolium*	0.495	114	*Knema hookeriana*	0.550
31	*Canarium littorale*	0.540	115	*Knema patentinervia*	0.530
32	*Canarium pseudodecumanum*	0.540	116	*Kokoona littoralis*	0.570
33	*Canarium schweinfurthii*	0.290	117	*Kokoona reflexa*	0.570
34	*Carallia brachiata*	0.570	118	*Koompassia excelsa*	0.630
35	*Castanopsis acuminatissima*	0.590	119	*Koompassia malaccensis*	0.760
36	*Cinnamomum iners*	0.499	120	*Kurgkur spp*	0.570
37	*Cryptocarya griffithiana*	0.510	121	*Lauraceae*	0.570
38	*Dactylocladus stenostachys*	0.610	122	*Lepisanthes alata*	0.570
39	*Dialium platysepalum*	0.763	123	*Lithocarpus amygdalifolius*	0.684
40	*Lithocarpus celebicus*	0.680	124	*Phaeanthus ophthalmicus*	0.570
41	*Lithocarpus spp.*	0.684	125	*Pokok Nyatoh Tembaga*	0.570

42	*Litsea castanea*	0.360
43	*Litsea costata*	0.360
44	*Litsea curtisii*	0.414
45	*Litsea elliptica*	0.414
46	*Litsea glutinosa*	0.414
47	*Litsea grandis*	0.414
48	*Lophopetalum javanicum*	0.570
49	*lrvingia malayana*	0.570
50	*lxonanthes icosandra*	0.696
51	*Macaranga gigantea*	0.295
52	*Macaranga spp.*	0.371
53	*Macaranga triloba*	0.371
54	*Maclurodendron porteri*	0.570
55	*Madhuca malaccensis*	0.960
56	*Melicope ptelefolia*	0.570
57	*Memecylon edule*	0.783
58	*Memecylon edule*	0.783
59	*Memecylon garcinioides*	0.783
60	*Memecylon pubescens*	0.783
61	*Mentimum spp*	0.783
62	*Mesua grandis*	0.711
63	*Metadina trichotoma*	0.720
64	*Mezettia leptopoda*	0.570
65	*Millettia atropurpurea*	0.570
66	*Mollatus spp.*	0.570
67	*Monocarpia marginalis*	0.570
68	*Myrisfica maxina*	0.570
69	*Myristicaceae*	0.570
70	*Nephelium juglandifolium*	0.776
71	*Nipperocapre venucolus*	0.570
72	*Nyatoh Nayke kuning*	0.570
73	*Nyatoh tembaga*	0.570
74	*Ochanostachys amentacea*	0.770
75	*Palaquium gutta*	0.615
76	*Palaquium hispidum*	0.589
77	*Pangium edule*	0.589
78	*Papaina obscura*	0.570
79	*Parkia speciosa*	0.570
80	*paropsia reliciformis*	0.570
81	*Paropsia verruciformis*	0.570
82	*Pela calyxyia*	0.570
83	*Pellacalyx axillaris*	0.380
84	*Pertusadina eurhyncha*	0.570
126	*Polyalthia rumphii*	0.570
127	*Polylthia glauca*	0.570
128	*Pometia pinnata*	0.653
129	*Porterandia anisophylla*	0.550
130	*Pouteria malaccensis*	0.660
131	*Pternandra echinata*	0.525
132	*Pterospermum spp*	0.570
133	*Rambutan xerospermum*	0.789
134	*Rhodamnia cinerea*	0.870
135	*Sandaricum koetjape*	0.473
136	*Sangal lofong*	0.570
137	*Santiria laevigata*	0.570
138	*Sapium baccatum*	0.335
139	*Scaphium macropodum*	0.530
140	*Scleropyrum wathchianuni*	0.570
141	*Shorea acuminata*	0.420
142	*Shorea bracteolata*	0.535
143	*Shorea hypochra*	0.615
144	*Shorea parvifolia*	0.405
145	*Sial Menahun*	0.570
146	*Spondias Dulcis*	0.570
147	*Sterculia foetida*	0.365
148	*Sterculia parvifolia*	0.365
149	*Streblus elongatus*	0.825
150	*Strombosia javanica*	0.527
151	*Styrax paralleloneurum*	0.570
152	*Sugi*	0.570
153	*Syzgium grande*	0.623
154	*Syzygium effusum*	0.623
155	*Syzygium griffithii*	0.623
156	*Syzygium malaccense*	0.623
157	*Syzygium myrtifolium*	0.623
158	*Syzygium spp*	0.623
159	*Tachyphyrnium grifJithii*	0.570
160	*Telang Kelawar*	0.570
161	*Terminalia subspathulata*	0.570
162	*Vitex pinnata*	0.460
163	*Xanthophyllum vitellinum*	0.709
164	*Xerospermum noronhianum*	0.770
165	*Xylopia ferruginea*	0.350
166	*Xylotria javanica*	0.536
167	*Litsea glutinosa*	0.570
168	*Paropsia verruciformis*	0.570

Appendix 9: Field photographs